

BAW-2241

April 1997

*THE
B&W*

OWNERS GROUP

Materials Committee

**Fluence and Uncertainty
Methodologies**

9705220079 970514
PDR TOPRP EMVBW
B PDR



**FRAMATOME
TECHNOLOGIES**

Framatome Technologies
Lynchburg, Va, 24506

Topical Report BAW-2241
Original Issue
April, 1997

Fluence and Uncertainty Methodologies

J. R. Worsham III, S. Q. King, and M. A. Rutherford

Abstract

Numerous improvements and updates have been made in the FTI fluence and uncertainty methodologies that are used to calculate the fast neutron fluence in the reactor system, particularly in the vessel materials and welds. These improvements and updates were made to enhance the accurate determination of vessel fluence and to establish a statistically sound methodology for estimating the bias and uncertainty in the calculated fluence. The methodology presented herein is calculation-based. Dosimetry measurements are not used in any way to determine fluence magnitude; they are used only to estimate biases and uncertainties. The results of B&WOG Cavity Dosimetry Benchmark Experiment were used in the update of the measurement biases and uncertainties for the entire FTI dosimetry database, and in the development of calculational biases and uncertainties. Pertinent excerpts of the experimental results are presented in this topical report.

Framatome Technologies, Inc.

RECORD OF REVISION

<u>Rev. No.</u>	<u>Change Section/paragraph</u>	<u>Description of Change</u>
0		Initial Release

Framatome Technologies, Inc.

Table of Contents

<u>Section</u>	<u>Page</u>
1.0 Introduction	1-1
2.0 Background	2-1
3.0 Semi-Analytical (Calculational) Methodology	3-1
4.0 Experimental Setup for Davis - Besse Cavity Dosimetry	4-1
5.0 Measurement Methodology	5-1
6.0 Measurement to Calculational Ratios of Dosimeter Responses	6-1
7.0 Uncertainty Methodology	7-1
7.1 Dosimetry Measurement Biases and Standard Deviations	7-7
7.2 Dosimetry Calculational Biases and Standard Deviations	7-23
7.3 Vessel Fluence Standard Deviations	7-36
8.0 References	8-1

-CONTINUED -

Appendix A

A-1

Appendix B

B-1

Appendix C

C-1

1.0 Introduction

The utilities that own and operate Babcock and Wilcox (B & W) reactors are entering a new phase of monitoring and evaluating the neutron fluence irradiation as it affects the degradation of the mechanical properties of their reactor vessel steels and welds. This new phase represents significant technological improvements over the previous methods used to determine vessel fluences:

1. The vessel fluences are predicted using calculated results from an analytical methodology.
2. Cavity dosimetry has been installed in each operating plant.¹
3. The uncertainty in the dosimetry measurements has been reevaluated and verified to be unbiased and has a standard deviation of 7.0 percent or less.
4. The uncertainty in benchmark comparisons of calculated to measured dosimetry results has been updated to include 35 capsule analyses, including 2 from the PCA "Blind Test", a comprehensive cavity benchmark experiment, and 3 standard cavity analyses.
5. The calculated capsule specimen fluence uncertainty is unbiased and has a standard deviation of 7.0 percent or less. The calculated vessel fluence uncertainty at an extrapolated end of life has a standard deviation that is less than 20.0 percent with appropriate monitoring.

These improvements are derived from the results of the B & W Owners Group (B&WOG) Cavity Dosimetry Program. The dosimetry program had three objectives:

1. Develop a methodology to accurately monitor the neutron fluence throughout the reactor core, internals, vessel, and cavity shield and support structure using neutron transport calculations validated by benchmarks to

Framatome Technologies Inc.

cavity dosimetry measurements.

2. Develop an uncertainty methodology consistent with the fluence methodology that provides appropriate estimates of the systematic and random deviations.
3. Evaluate the dosimeter types that could be utilized in the vessel cavity regions to provide adequate measurements for benchmarking the calculations.

The program was completed in 1992, and in July a meeting was held with the United States Nuclear Regulatory Commission (NRC). The NRC raised two issues in their preliminary review of the results. The first was that the NRC's previously recommended cross section library, BUGLE-80², was biased (which was clearly confirmed by the results from the "Benchmark Experiment" part of the "Cavity Dosimetry Program"). The second issue was that the NRC was concerned with the vessel fluence uncertainties being consistent with the Pressurized Thermal Shock Safety Analysis^{3, 4, 5} and screening criteria⁶ without an analytical modeling of the uncertainties. The B&WOG decided to update the cavity dosimetry program before submitting a fluence topical to the NRC. The update consisted of (1) a reanalysis of the Benchmark Experiment using the NRC's latest recommended library, BUGLE-93⁷, and (2) a new uncertainty evaluation that integrated (a) an analytical vessel fluence uncertainty, (b) cavity and capsule benchmarks, and (c) the Cavity Dosimetry Program reevaluation of the measurement uncertainty,

In 1993, before the updates to the Cavity Dosimetry Program could be completed, the NRC issued Draft Regulatory Guide DG-1025, "Calculational And Dosimetry Methods For Determining Pressure Vessel Neutron Fluence",⁸ which outlined the requirements for comprehensive analytical, benchmark, and measurement fluence uncertainties. The B&WOG and Framatome Technologies, Inc. (FTI) provided the NRC with comments and suggestions to make the draft regulatory guide more useful. The comments noted that the

Framatome Technologies Inc.

B&WOG and FTI would appropriately modify their fluence and uncertainty methodologies to satisfy the guide when it was issued as a Regulatory Guide. As discussed in Sections 2.4.3 and 3.0, the fluence methodology has been changed to a Semi - Analytical BUGLE-93 method. In this method, the fluence results are absolute, best-estimate calculations, with no plant - specific adjustments. FTI has defined a program for the B&WOG to evaluate the measurement, benchmark, and analytical uncertainty requirements of the guide. However, the draft guide contains more requirements than those outlined by the NRC for the Cavity Dosimetry Program, and in June of 1996, the draft guide was reissued for comments (as DG-1053).¹⁹

The B & W Owners and FTI will evaluate the draft guide uncertainty requirements when they become part of a Regulatory Guide. In the interim period however, before the draft guide is finalized, most of the owners will be updating their reactor coolant system pressure - temperature limits for heat-ups and cool-downs. In addition, most owners will be revalidating the analytical monitoring of their vessels by performing vessel fluence analyses that include absolute calculations of the fluence and benchmark comparisons of the calculations to cavity dosimetry measurements. Since the methodology for validating the calculations with benchmark comparisons to cavity dosimetry measurements represents a significant technological improvement over the previous methodology,⁹ and the Benchmark Experiment provides an update of the measurement uncertainty as well as an update of the benchmark uncertainty, the B&WOG has funded the preparation of this topical report.

This report describes five significant technological improvements. These improvements incorporate many of the requirements noted in the draft guide, such as the requirement that the vessel fluence predictions be determined completely from calculations without any adjustments or normalization to each plant specific measurement. However, some of the new draft guide requirements, such as the comprehensive evaluation of an analytical uncertainty model to estimate the vessel fluence uncertainty and the comprehensive

Framatome Technologies Inc.

statistical evaluations of benchmarks to determine the calculational bias have not been incorporated into this topical. The B & W Owners do not believe that it is cost effective to update these evaluations at this time. Therefore, the analytical uncertainty model is based on an update of the previous evaluations,^{9, 10, 11, 12} and the benchmarks are based on an update of the greater than 0.1 MeV (million electron Volts) weighted fluence response functions. When the draft guide is issued in final form, the uncertainty evaluations will be reassessed to determine if they comply with the guide, and if a revised topical report is needed.

2.0 Background

The purpose of this topical report is to (a) describe the Framatome Technologies, Inc. (FTI) improved methodology for predicting the fluence throughout the reactor and vessel cavity structure, and (b) describe the corresponding uncertainty methodology for estimating the bias and standard deviation in the fluence predictions. The methodologies that will be discussed follow a history of nearly thirty years of technological improvements. This is the fifth in the series of topical reports describing the improvements.^{9,12,13,14} The reasons for the earlier improvements were to increase the accuracy and to reduce the uncertainty in the fluence predictions for the vessel and weld material specimens. These most recent improvements are to increase the accuracy of the fluence predictions and verify the fluence uncertainty for the actual vessel material and welds, rather than that of the capsule specimens of vessel and weld materials.

2.1 Irradiation Embrittlement 1950's - 1977

Accuracy and precision in the predictions of the vessel fluence are important in order to accurately and precisely determine the neutron irradiation effects upon vessel materials. Since the late 1950's it has been known that relatively low levels of neutron irradiation could degrade the mechanical properties of the steels and welds used in the fabrication of reactor vessels. The degradation appeared to be the result of an increase in embrittlement. However, the phenomenon was difficult to understand because it varied significantly from one type of steel to another, one heat treatment to another and one weld to another. Research and development programs were initiated to better understand the irradiation embrittlement phenomenon. In 1961, the American Society for Testing and Materials established a standard for reactor vessel surveillance programs (ASTM E 185-61, "Standard Practice for Conducting Surveillance Tests for Light-Water Cooled Nuclear Power Reactor Vessels"). FTI (formerly Babcock and Wilcox) developed a surveillance program to monitor the changes in the mechanical properties of vessel

material test specimens for each reactor that was in accordance with the ASTM standard.

By the late 1960's, the Naval Research Laboratory had discovered that copper and phosphorus were the elements that most significantly affected the irradiation embrittlement process. However, the accuracy and reliability of the empirical techniques used to evaluate the irradiation damage to vessel materials were poor. In 1973, the NRC implemented 10 CFR 50, Appendix G, "Fracture Toughness Requirements" and 10 CFR 50 Appendix H, "Reactor Vessel Material Surveillance Program Requirements" to improve the quality of predictions of irradiation damage by relying on the theoretical concepts of fracture mechanics rather than on empirical techniques.

2.2 Dosimetry Improvement 1977 - 1992

When Charpy specimens from the surveillance programs in operating reactors began to be available in sufficient quantity, correlations of the data resulted in large uncertainties in the predictions of embrittlement (ΔRT_{NDT}). The uncertainties in the correlated predictions were due in part to the uncertainties in the predictions of the integral of the neutron fluence (ϕt) over time, where ϕ is the neutron flux with an energy greater than 1.0 MeV and t is the total time of neutron irradiation. FTI recognized that the industry needed an accurate and consistent methodology for predicting Charpy specimen fluences. Therefore, in concert with the "Light Water Reactor Pressure Vessel Surveillance Dosimetry Improvement Program" that the NRC program initiated in 1977 to improve dosimetry measurement predictions, FTI developed the most technologically advanced methods for performing dosimetry measurements and fluence analyses. The accuracy and consistency of the FTI methods were independently confirmed by R.L. Simons, E.P. Lippincott, et alia, from the Westinghouse Hanford Company.¹⁵

Table 2-1 shows the standard deviations in the adjustments that Simons made to have the industry predictions of capsule fluence values be consistent.

Table 2-1

Standard Deviations In The Fluence Adjustments¹⁵ For Reg. Guide 1.99, Rev. 2

<u>Capsule</u>	<u>Standard Deviation (%)</u>
Westinghouse	29.7
CE	24.2
B & W	5.6

Clearly, the FTI methodology produced very precise fluence predictions. The precision in the FTI results, and Simons' adjustment of the other capsule fluences, provided fracture mechanics analysts with the means of analyzing reactor vessel materials to ensure (1) sufficient margin for nonbrittle behavior, and (2) minimal probability of a rapidly propagating fracture.¹⁷ The FTI fluence analysis methodology has satisfied the basic requirements of 10 CFR 50, Appendices G and H, with respect to vessel material test specimens. However, the NRC and some industry experts have expressed reservations about the fluence methodologies used by various analysts in the industry.

The reservations have focused on the requirements for vessel evaluations rather than specimen evaluations. The basic vessel uncertainty requirements are defined by the Pressurized Thermal Shock (PTS) Safety Analyses.^{3, 4, 5} The PTS Safety Analyses are based on probabilistic evaluations of overcooling transients. The results of these analyses are defined in terms of a 95 percent probability that the mean frequency of PTS events causing vessels to crack is within 10 percent of 5×10^{-6} per reactor year, if RT_{PTS} is not greater than the 10 CFR 50.61⁶ screening criteria. The fluence uncertainty associated with the safety analyses is assumed to be that estimated by Simons¹⁵ for the embrittlement to fluence correlation.^{16, 17} The root mean square standard deviation of Simons measured fluences is 21 percent. The NRC has defined acceptable values of the fluence uncertainty to be 20 percent⁸ or less to maintain consistency with the PTS screening criteria⁶ and the

Regulatory Guide 1.99, Revision 2 embrittlement correlation.¹⁷

Reviewing Table 2-1 clearly shows why the NRC and some industry experts have expressed reservations about the fluence uncertainty. Fluence predictions for Westinghouse and CE capsules have adjustments with standard deviations that are larger than the acceptable uncertainty. For Westinghouse capsules, more than 55 percent of the original fluence predictions required a greater than 20 percent adjustment to be consistent with the industry. While the NRC's acceptable uncertainty for the industry may be no more than 20 percent, the average value in Table 2-1 is clearly lowered by the FTI results. If embrittlement correlations for safety analysis are based on a 20 percent standard deviation, there is clearly a concern that industry analyses of Westinghouse and CE capsules are not within the 20 percent criteria. However, the B & W standard deviation of 5.6 percent indicates that the FTI fluence predictions are very accurate, and much smaller than the 20 percent criterion.

As noted above, the accuracy and reliability of the FTI fluence methodology was established in concert with the NRC's "LWR Pressure Vessel Surveillance Dosimetry Improvement Program." When this program was initiated in 1977, the NRC needed to know the uncertainties in the capsule fluence predictions in order to develop an industry embrittlement correlation suitable for safety analyses. With the limited data available, FTI found that the only uncertainties that could be estimated with any confidence were bounding values. Therefore, FTI provided the NRC and its contractors with capsule specimen embrittlement data, fluence predictions, and the bounding capsule fluence uncertainties derived from measured dosimetry activities and response functions. The bounding uncertainty value for the capsule measurements is 15 percent as shown in Reference 12. The bounding values of the fluence uncertainties subsequently became the FTI standard set. This set was accepted by the NRC as referenced in the "Integrated Reactor Vessel Material Surveillance Program".¹⁰

Framatome Technologies Inc.

2.3 Licensing Basis 1977 - Present (1997)

The NRC Safety Evaluation of the integrated surveillance program states:¹⁰

Uncertainties in neutron fluence estimates were discussed by the staff in its review of the B & W owners group request for exemptions to the requirements of Appendix H, 10 CFR 50. The dosimetry methodology and vessel fluence analysis have been reviewed and accepted by the staff in a memorandum dated December 5, 1984 from L.S. Rubenstein to W.V. Johnston, "Review of Response to the Request for Additional Information on Capsule RSI-B for Rancho Seco, Reported in BAW-1702."

In the staff's review of BAW-1702 it was reported that this methodology resulted in a maximum uncertainty in end-of-life vessel fluence of 34 percent. This uncertainty may be reduced for vessels not containing in-vessel dosimetry by inclusion of dosimetry devices in the reactor cavity. The B & W Owners Group has indicated that they have begun testing of these types of dosimeter devices. However, until these devices are installed, plants without dosimetry in the reactor vessel will have to rely on the methods of neutron fluence analysis documented in BAW 1702.

The NRC Evaluation of BAW-1702 provided the following table:¹¹

Table 2-2

FLUENCE CALCULATION UNCERTAINTY

<u>Calculation</u>	<u>Uncertainty %</u>
	Without

Framatome Technologies Inc.

	<u>Capsule Rotation</u>	<u>With Capsule Rotation</u>
<i>Capsule (derived from measured activity)</i>	± 14	± 15
<i>Pressure vessel (maximum location for capsule irradiation time interval)</i>	± 20	± 21
<i>Pressure vessel (maximum location, long term extrapolation)</i>	± 22	± 23
<i>Pressure vessel welds</i>	± 33	± 34

CONCLUSION

We have reviewed the Sacramento Municipal Utility District response dated September 27, 1984 regarding Rancho Seco surveillance capsule dosimetry. Due to the capsule rotation the computational uncertainty of the flux as applied to the maximum location of the pressure weld should be increased by a small amount i.e., from $\pm 33.0\%$ to $\pm 34.0\%$.

FTI's standard uncertainties in Table 2-2 are based on bounding values that were first documented in 1978.¹² Since 1978, the NRC and its contractors have performed (1) a least squares adjustment of the capsule fluence values to obtain an industry consistent set,¹⁵ (2) a least squares correlation of capsule embrittlement measurements to the industry consistent capsule fluence values,¹⁶ and (3) generic pressurized thermal shock (PTS) safety analysis of Westinghouse,⁵ CE,⁴ and B & W³ reactors using probabilistic fracture mechanics analyses of the effects of rapid overcooling transients. In each of the three

Framatome Technologies Inc.

analyses performed for the NRC (fluence adjustments, embrittlement correlations and generic safety analyses), fluence uncertainties were estimated and appropriately treated. However, the uncertainties were not estimated in terms of bounding values, but rather as standard deviations. Therefore, there is a confidence factor difference between the bounding FTI standard fluence uncertainties and the value that the NRC assumed for PTS evaluations and coolant system pressure - temperature embrittlement evaluations.

A confidence factor with a value of 2.0 is used in the PTS safety analysis. This confidence factor provides a 95 percent probability that the risk of vessel failure due to PTS events is acceptable for any plant as long as the value of RT_{PTS} is below the PTS screening criteria.⁶ A confidence factor of 2 is also used in the Regulatory Guide 1.99¹⁷ "Margin" term. Therefore, the bounding fluence uncertainties that are consistent with the PTS screening criteria,⁶ Regulatory Guide 1.99¹⁷, and the FTI standard set, would be less than or equal to 40 percent. This is the value that is assumed for NRC evaluations and approval of the FTI set of standard uncertainties in Table 2-2.

2.3.1 Reference Fluence Methodology

Prior to 1973, the FTI fluence methodology was based on one-dimensional diffusion theory for spatial neutron transport with multigroup removal cross sections corrected for anisotropic effects.¹⁴ By 1973, when the NRC added Appendices G and H to the Federal Register (10 CFR 50), FTI had expanded their analytical capabilities by adding the ANISN and DOT computer codes to the fluence methodology.¹³ The cross section library had also been updated to the CASK data set.¹⁸ This data provided anisotropic scattering cross sections with a P_3 Legendre expansion of the energy - angular variables.

The analysis of capsule dosimetry and the predictions of material specimen fluences began in 1976. At that time, the "Reference Fluence Methodology" included DOT - II W, with radial (r) and theta (θ) coordinates modeling the radial plane of the reactor, S_6 quadrature for the angular flux expansion, and CASK cross sections with a P_1 expansion of the angular scattering. The P_1 DOT results were modified by the ratio of P_3 to P_1 ANISN results. The source of neutrons was represented by a two - dimensional distribution of fission rates in each fuel pin integrated over the appropriate operational period with a U-235 fission spectrum. The synthesis of the r, θ DOT results to three - dimensions (r, θ, z) was accomplished with the results from a three - dimensional nodal diffusion theory computer code that explicitly modeled the peripheral fuel assemblies throughout the operational period. The normalized shape of the fission power in the axial (z) direction provided the functional distribution of the time-averaged flux from the core periphery to the vessel.

The capsule analysis utilized cell theory to treat the geometrical modeling in an independent DOT calculation of an azimuthal segment with rectangular coordinates. The time-averaged flux spectrum for the dosimetry and material specimens was found to be sufficiently representative of the spectrum at the center of the capsule. Therefore, comparisons of measured dosimeter activities to calculated activities were based on integrated averages at the center of the capsule. The integration of time dependent functions, such as fission rates, and isotopic production and decay, included the appropriate dependencies such that comparisons of measurements and calculations were functionally equivalent in time.

This model is described in the Reference 12 topical report. It was the basis for the capsule fluences using appropriate weighting of the dosimetry measurements. The uncertainties in the measured activities were determined to be unbiased, but in attempting

to define the standard deviation, there were too few independent capsule measurements (only six) to confirm that the distribution in the deviations was sufficiently normal. Therefore, bounding values of the uncertainties were estimated. The bounding values,¹² and those in Table 2-2 are essentially the same.

The comparisons of calculated activities to measured values averaged less than 10 percent in the energy range around 1.0 MeV. With the bounding uncertainty in the measured activities being estimated as 15 percent or less, it was not possible to identify any separate biases in the calculations. Therefore, the calculated and measured fluences with an energy greater than 1.0 MeV at the capsule were the same values. The capsule fluences were defined as measured values for application to embrittlement analyses. The bounding uncertainty (2 standard deviations) in the capsule fluences was estimated as the statistically combined uncertainties for the measured activities (15 percent) and the activation cross sections (11 percent). Thus, the "measured" fluence at the capsule, with energies greater than 1.0 MeV, was defined to have an uncertainty of 19 percent or less.

The vessel fluence was determined using a modification to the DOT calculational methodology just described. The modification utilized a cylindrical (r, z) geometrical model with the appropriate source of neutrons from the three - dimensional fission rates. The cylindrical coordinates provided a symmetrical three - dimensional model of the vessel beltline region. Asymmetries in the fission source distribution and core former region were evaluated from the planar (r, θ) DOT results. Since the capsule calculations of the dosimetry indicated agreement between the calculations and measurements within the measurement uncertainty, the vessel fluences were defined as measured values with combined measurement and analytical uncertainties.

2.3.2 Methodology Validation

In 1977, when the NRC established their "Light Water Reactor Pressure Vessel Surveillance Dosimetry Improvement Program", one part of this program was to test the industry to evaluate the overall bias and uncertainty in the fluence predictions. To ensure that the evaluation actually represented the bias and uncertainty from each participant, the test was developed to be a "blind test". This meant that the participants would not know the measurement results before everyone had submitted their calculational results. The Pool Critical Assembly (PCA) blind test was supervised by the Oak Ridge National Laboratory (ORNL).³⁷ FTI and the other industry participants modeled the PCA reactor and predicted dosimetry activations in the vessel and internals structure. FTI submitted their calculations to ORNL, and ORNL compared FTI's calculations (*C*) to their measurements (*M*) and sent FTI the *C/M* results along with the assessment of their measurement uncertainty. The *C/M* results indicated a mean deviation of 6.7 percent. The ORNL measurement uncertainty was between 6.0 percent and 10.0 percent. These uncertainty results were the best of all participants, including Oak Ridge and the Brookhaven National Laboratory, who already knew the measured results.³⁷

Since 1976, there have been six revisions, or modifications, to update the fluence methodology. This topical report describes the fifth and sixth revisions in detail. Sections 2.3.3 through 2.3.6 briefly outline the first two revisions and the first two modifications. The four previous methodologies are:

- 1) Semi - Empirical
- 2) Semi - Empirical BUGLE-80
- 3) Measurement - Based
- 4) Hand - Adjoint

The fifth and sixth updated methodologies are:

- 5) Semi - Analytical BUGLE-80
- 6) Semi - Analytical BUGLE-93

Only the Reference (Section 2.3.1, page 2 - 8), Semi - Empirical and Semi - Empirical BUGLE-80 methodologies are consistent with the uncertainties reviewed in this topical and described in Table 2-2.

2.3.3 Semi - Empirical

The methods, procedures, and computer modeling that comprise the Semi - Empirical methodology are described in Reference 9. This methodology was completed by 1980 and was used for the PCA blind test calculations. The significant differences from the reference methodology are: (1) updates of the DOT code, (2) P_3 scattering and an S_8 quadrature directly in the DOT model, (3) corrections for short half-lives, photofissions and fissile impurities associated with the dosimetry comparisons, (4) the synthesis of the vessel beltline fluence used the axial distribution of the three-dimensional fission rate, (5) the combination of activities to determine the greater than 1.0 MeV measured fluence applied equal weighting to the U-238, Np-237, Ni-58 and Fe-54 dosimeters, and (6) the M/C ratio of activities for the four dosimeters responding above 1.0 MeV provided a normalization to convert calculated fluences to measured ones. The M/C normalization was applied to calculated capsule fluences to represent measured fluences even though the C/M ratios never indicated a bias in the calculations. The M/C ratios were only applied to predictions of vessel fluences if the ratio was greater than one (1.0). This methodology was used until 1990 when it was phased out and replaced by the Semi - Empirical BUGLE-80 methodology.

2.3.4 Measurement - Based

In 1983, the Semi - Empirical methodology was simplified and reduced to the Measurement - Based methodology. The development of the Measurement - Based methodology involved averaging the calculational results from the Semi - Empirical

methodology and treating them as constants. The two key constants were the dosimeter activation response functions and the vessel lead factors. The lead factors represented the ratio of the greater than 1.0 MeV flux at the capsule to the vessel flux at weld and other important locations.⁹ If the spectral and spatial distribution of the neutrons from the fission source remained constant, then this methodology would be equivalent to the Semi - Empirical and notably simpler. However, the (reactor) core fuel management changed dramatically in the ensuing years to the Framatome Cogema Fuel Company's invention of the low leakage fuel loading scheme. Consequently, the spectral and spatial distribution of the neutrons changed significantly and the uncertainties in the results of the Measurement - Based methodology were unknown. In Reference 9, an estimate of 50 percent uncertainty was judged to be appropriate.

This methodology was discontinued in 1986 after the analyses of six capsules. These capsules are not included in the fluence uncertainty database.

2.3.5 Semi - Empirical BUGLE-80

By 1990, the calculations of the B & W Owners Group Cavity Dosimetry Benchmark Program had begun. The program incorporated two calculational analyses of the dosimetry. The two calculational methods, procedures, and computer models were identical with the exception that one analysis used the CASK library¹⁸ and the other used the BUGLE-80 library². The results of the *C/M* benchmark comparisons for the capsules indicated that no independent bias could be determined with BUGLE-80 and that the standard deviation in the BUGLE-80 calculations was equivalent to the standard deviation in the CASK calculations.

The results of *C/M* benchmark comparisons for the cavity dosimetry indicated that the BUGLE-80 library resulted in a large bias in the calculations. However, since the capsule calculations had no bias and had a standard deviation comparable to previous results, the Semi - Empirical BUGLE-80 methodology was used for fluence predictions

of capsules and the vessel inside surface. The uncertainties were within FTI's standard set of values in Table 2-2.

2.3.6 Hand - Adjoint

In 1990, the B & W Owners Group had FTI develop the Hand - Adjoint methodology for predicting changes in the fluence due to fuel management changes. This methodology was designed to quickly update the predicted reactor vessel fluence at the end of life (EOL) whenever a new fuel cycle design was implemented that differed from the reference design used to predict the fluences at EOL. The methodology is based on using adjoint calculations with the Semi - Empirical (CASK) methodology to define constant factors that relate peripheral assembly fission rates to specific vessel locations. The methodology has no defined uncertainty because it is not intended for predicting the fluence. The methodology simply provides a means of estimating the effect of fuel management changes on vessel fluence. Since the Hand-Adjoint methodology is not intended for fluence predictions, no benchmark comparisons of calculations to measurements in the FTI database utilize this methodology.

2.4 NRC Issues

The five improvements to the fifth and sixth FTI fluence methodologies and associated uncertainties (page 1 - 1) that are presented in this topical report address the following outstanding issues that FTI and the NRC have discussed since 1985:

- 1) Vessel Surveillance
- 2) Measurement Uncertainties
- 3) Calculated Fluences
- 4) Update of Benchmarks

There is a fifth outstanding issue concerning additional uncertainty evaluations discussed in Draft Regulatory Guide DG-1053.¹⁹ As noted previously, FTI and the B & W

Owners view most of the provisions in the draft as improvements to plant safety. Therefore, the intention is to incorporate these provisions into the fluence and fluence uncertainty methodologies. However, because the draft is in the review process, and this topical report needs to address the B & W Owners update of their pressure - temperature limits for heat-up and cool-down, this report does not address the additional draft regulatory guide uncertainty evaluations. The four NRC issues are briefly reviewed in the following subsections.

2.4.1 Vessel Surveillance

In 1976, several owners of B & W reactors found that the surveillance capsule holder tubes had been damaged during operation. The damage necessitated the removal of the holder tubes. While replacement of the holder tubes was an option, it was a poor one in comparison with the Integrated Reactor Vessel Material Surveillance Program.¹⁰ The integrated program utilized similar reactors with holder tubes to irradiate vessel material specimens from reactors without them. In addition, the NRC granted the reactors without holder tubes an exemption from Appendix H requirements for a period of five years. During this period, a cavity dosimetry program was developed with vessel monitoring conducted by calculational evaluations.

The Cavity Dosimetry Program was presented to the NRC in a topical report in 1986.²⁰ By 1990, all B & W Owners had installed dosimeters in the cavities of their reactors. While these dosimeters cannot provide an active role in surveillance (because the fluxes that reach the cavity have different spectra and lower levels than the key locations at the surface and one-quarter thickness of the vessel), these dosimeters provide results for benchmarking the calculations. Calculational evaluations of vessel fluences continue to provide the monitoring required for vessel surveillance. Periodic vessel surveillance updates include benchmarks to dosimetry to verify that the accuracy and uncertainty in the calculations continues to be within the reference values noted in Section 7.0 .

The vessel surveillance program, to ensure appropriate monitoring for extrapolated projections of the fluence for the reactor coolant system pressure - temperature curves and the end of life PTS criteria, is not addressed in this topical.

2.4.2 Measurement Uncertainties

When FTI provided the NRC with the topical report describing the "Integrated Reactor Vessel Material Surveillance Program" in 1985,¹⁰ uncertainties in the neutron fluence estimates were discussed with the staff. The NRC approved the values provided in Table 2-2. However, in 1988, when FTI submitted Revision 1 of the topical, "Pressure Vessel Fluence Analysis for 177-FA Reactors",⁹ the NRC questioned the measured fluence uncertainties. The documentation referencing the laboratory uncertainties could not be independently verified. Therefore, the NRC's question concerning the measured fluence uncertainties remained an open issue even though the uncertainty values noted in Table 2-2 remained as the basis for safety and licensing analyses using FTI fluence predictions.

The B & W Owners Group Cavity Dosimetry Program included a reevaluation of the measurement uncertainties (Section 7.1). Not only was each step of the experimental process reviewed to estimate the uncertainties in the equipment and procedures, but each step was independently reviewed by W. N. (Bill) McElroy and R. (Ray) Gold as noted in their "Written Comments and Recommendations Related to the Review of the B&WOG (B & W Owners Group) Davis-Besse Cavity Dosimetry Benchmark Program".²¹ The Quality Assurance verification of the experimental methodology and the independent review by the consultants indicated that the values in Table 2-2 are greater than the measurement standard deviation by a confidence factor of 2.0. This implies that there is a 95 percent probability that the measurement uncertainties in Table 2-2 bound the uncertainties for any plant specific evaluation.

2.4.3 Calculated Fluences

In February of 1993, the NRC had a meeting with industry representatives. At the meeting, the NRC explained that various experts have expressed concerns that the uncertainty in the fluence predictions may be inconsistent with the Pressurized Thermal Shock (PTS) Safety Analyses.²² By September of 1993, the NRC had released Draft Regulatory Guide DG-1025 which explained that the current technology for determining reactor vessel fluences based on dosimetry measurements needed updating. A key feature of the draft guide is that vessel fluence predictions must be based on calculations. Extrapolations of measured fluences are not acceptable.

FTI evaluated the fluence treatment in the generic PTS Safety Analyses²² and found that the probabilistic analyses of overcooling transients, embrittlement uncertainties and fluence uncertainties are a concern with respect to measurement based fluence predictions. The concern is that the PTS analyses are based on a 95 percent probability that the mean frequency for through-wall crack penetration is less than 5×10^{-6} per reactor year. Consequently, the measured vessel fluences must have an uncertainty that is consistent with the 95 percent probability. However, there are no vessel fluence measurements. Without such data, it is difficult to ensure that the "measured" vessel fluences are within 95 percent tolerance limits of the true predictions. Therefore, it is also difficult to ensure that vessel embrittlement predictions are consistent with the PTS Safety Analyses.

To enhance the safety of vessel embrittlement evaluations, FTI is changing the fluence methodology from the Semi - Empirical measurement based technology to the Semi - Analytical calculational based technology. As discussed in Section 2.3.3, the Semi - Empirical methodology has no bias between the calculations and measurements, therefore the calculated fluence with energies greater than 1.0 MeV equaled the measured fluence. The calculated fluences for each plant specific analysis were normalized to the measurements. The measured fluence uncertainties could thereby be estimated in terms of the uncertainties in the experimental methodology and the uncertainties in the dosimeter response functions.

The change from the Semi - Empirical, measurement based methodology to the Semi - Analytical, calculational based methodology is the principal topic described in this report. The effects on previous capsule and vessel fluence predictions are negligible in terms of any net bias (although some vessel fluence values may be too high). The effects on embrittlement correlations should be examined. The principle effects will be in the uncertainty methodology to estimate the standard deviation in the calculated fluence. The uncertainty methodology will be different from that previously used to estimate the bounding values in Table 2-2 (see Section 7.0).

2.4.4 Update of Benchmarks

When FTI submitted Revision 1 of the "Pressure Vessel Fluence Analysis for 177-FA Reactors" topical report to the NRC in 1988, the NRC wanted to see the entire database of capsule dosimetry to verify the uncertainty in the calculational benchmark to measurements. Because the topical never resolved the issue of measurement uncertainties, the entire database was never sent to the NRC. Again in 1995, the NRC was reviewing FTI fluence uncertainties associated with embrittlement predictions of Entergy Operations' Waterford reactor vessel and wanted to review the entire database. However, when Entergy reduced the period for their pressure - temperature technical specification limits for heat-up and cool-down from 20 effective full power years to 15, the NRC dropped their request for the database.

This topical report contains an update of the entire FTI database of capsule and cavity dosimetry measurements and calculations as shown in Table A-1. The capsule and cavity *C/M* benchmark results are summarized in Table A-2.

3.0 Semi - Analytical (Calculational) Methodology

SECTION 3 IS FTI PROPRIETARY

4.0 General Arrangement of Experiment

The Cavity Dosimetry Benchmark Experiment, also known as the In-Out Experiment, was a full-scale test conducted in the Davis-Besse Unit 1 B&W-designed 177 fuel assembly reactor, using both in-vessel and ex-vessel dosimetry. The dosimetry consisted of 23 RMs (243 activation foils or wires, 7 fission foils, and 33 flux mapping stainless steel chain segments), 6 SSTRs, 22 ultra-high purity niobium dosimeters, 4 HAFMS (3 beryllium and 1 lithium). The LiF chips are gamma fluence detectors and were specially developed by the National Institute of Standards and Technology (NIST) for this specific application to provide accurate results at the high exposure levels expected in this experiment. The dosimetry described above was provided by six program contributors - the B&W Owners Group; Hanford Engineering Development Laboratory (HEDL); Center for the Study of Nuclear Energy, Mol, Belgium (CEN/SCK); NIST; Rockwell International; and the Arkansas Technical University.

The in-vessel dosimetry consisted of two standard unirradiated TMI-2 surveillance capsules installed in the surveillance capsule holder tube at the peak flux (11°) location. (Throughout this document, unless otherwise stated, azimuthal positions are referenced to one of the four "major axes.") These capsules contained six standard B&W RM dosimeter sets covering incident neutron threshold energies from 0.5 eV to 2.5 MeV.

The cavity dosimetry consisted of sixteen specially fabricated aluminum dosimetry holders, each containing five sets of dosimeters. A detailed sketch of the cavity dosimetry holder is given in Figure 4-1, showing the numerical designation for each position of the canisters containing a set of dosimeters. Cable assemblies containing these holders were then designed in a manner that allowed for accurately known measurements of the dosimeter locations, maintaining the dosimetry in a known direction either facing towards or away from the core, and each installation and removal. Five cable assemblies containing the dosimeter holders at various axial positions were installed in the cavity at

specific azimuthal positions. The azimuthal locations were chosen to avoid possible areas of large flux gradients, which are difficult to predict analytically. Figure 4-2 shows the general arrangement of the cavity dosimetry holders. The assemblies at 6° , 11° , and 11.5° were located in the region of maximum flux, while the holder at 42.5° was in the minimum flux region. Table 4-1 details the dosimetry loaded in the holders by canister position. Note that dosimeters loaded in positions 1 and 2 were placed in aluminum cans and are unshielded, while dosimeters loaded in positions 3, 4, and 5 were placed in gadolinium²⁵ cans to shield them from the thermal flux.

Four 50 ft-long beaded stainless steel chains were also placed in the cavity region to achieve accurate axial flux profiles at the azimuthal positions of interest. The chain assemblies were mounted beneath Nuclear Instrumentation boxes in four of the open source check tube penetrations, one in each quadrant of the cavity. The chains were anchored with a heavy weight at the containment floor to limit lateral movement during plant operation. An additional 35 ft-long University of Arkansas stainless steel chain was suspended from the 11° train.

All 80 sets of dosimetry, stainless steel chains, and surveillance capsules were installed for one cycle of operation in the Davis-Besse Unit 1 plant and removed at the completion of cycle 6 in February 1990. The coordinate location dimensions of the cavity dosimetry holders are listed in Table 4-2, with the reference coordinate system presented in Figure 4-3. A plan view, Figure 4-4, is included showing the relative positions of the temporary cavity dosimetry assemblies, the permanent cavity dosimetry holder, the stainless steel chains, and the in-vessel standard surveillance capsules.

Table 4.1. Loading Plan of Cavity Dosimetry Holders

Holder and Location	Unshielded Positions 1, 2 (Aluminum Cases)	Shielded Positions 3, 4, 5 (Gadolinium Cases)
<p style="text-align: center;">A</p> <p>11.5° Seal Plate Elevation</p>	<p>1 - B&W RMs Fe Co</p> <p>2 - B&W RMs Fe Co</p>	<p>3 - LiF</p> <p>4 - B&W RMs Fe Co HAFM 3 Be Li</p> <p>5 - B&W RMs Fe Ni 3 Cu Co</p>
<p style="text-align: center;">B</p> <p>11.5° Nozzle Elevation</p>	<p>1 - HEDL RM</p> <p>2 - B&W RMs Fe Co</p> <p>B&W SSTR (2B)</p>	<p>3 - LiF</p> <p>4 - HEDL RM HEDL SSTR (23H)</p> <p>5 - B&W SSTR (2C2) B&W RMs Fe Ni 2 Cu Co</p>

<p style="text-align: center;">C 11.5° Nozzle Elevation</p>	<p>1 - B&W RMs Fe Co</p> <p>2 - B&W RMs Fe Co</p>	<p>3 - SS Chain #1</p> <p>4 - B&W RMs Fe Ni 2 Cu Co Nb (ToyoSoda) HAFM 3 Be Li</p>
---	---	--

Table 4.1. Loading Plan of Cavity Dosimetry Holders (Cont'd)

Holder and Location	Unshielded Positions 1, 2 (Aluminum Cases)	Shielded Positions 3, 4, 5 (Gadolinium Cases)
<p style="text-align: center;">D</p> <p>11.5° Upper Active Fuel Elevation</p>	<p>1 - HEDL RM</p> <p>2 - B&W RMs Fe Co B&W SSTR (EB)</p>	<p>3 - LiF</p> <p>4 - B&W RMs Fe Ni Cu Co</p> <p>5 - B&W SSTRs (3C, B&W-17) HEDL SSTR (Z2H) HEDL RM</p>
<p style="text-align: center;">E</p> <p>11.5° Upper Active Fuel Elevation</p>	<p>1 - B&W RMs Fe Co</p> <p>2 - SS Chain #2</p>	<p>3 - SS Chain #3</p> <p>4 - B&W RMs Fe Co Nb HAFM 3 Be 1 Li</p> <p>5 - B&W RMs</p>

<p style="text-align: center;">F</p> <p>11.5° Core Midplane Evaluation</p>	<p>1 - B&W RMs Fe Co PUD</p> <p>2 - B&W SSTR (4B) HEDL SSTR (A2H)</p>	<p>3 - B&W RMs Fe Ni Cu Co Nb (ToyoSoda) HAFM 3 Be Li Nb (MOL)</p> <p>4 - B&W SSTRs (4C, B&W-18) HEDL SSTR (A2H)</p> <p>5 - MOL RM</p>
--	---	--

Table 4.1 Loading Plan of Cavity Dosimeter Holders (Cont'd)

Holder and Location	Unshielded Positions 1, 2 (Aluminum Cases)	Shielded Positions 3, 4, 5 (Gadolinium Cases)
<p style="text-align: center;">G</p> <p>11.5° Core Midplane Elevation</p>	<p>1 - HEDL RM PUD</p> <p>2 - B&W RMs Fe Co Co-Al Wire Fe Wire PUD</p>	<p>3 - LiF</p> <p>4 - LiF</p> <p>5 - HEDL RM B&W RMs Ni Wire Co-Al Wire Np-Al Wire U-Al Wire</p>
<p style="text-align: center;">H</p> <p>42.5° Core Midplane Elevation</p>	<p>1 - B&W RMs Fe Co</p> <p>2 - SS Chain #4</p>	<p>3 - LiF</p> <p>4 - B&W RMs Fe Co Nb (ToyoSoda) HAFM 3 Be Li</p> <p>5 - SS Chain #5 U-238 Powder Np-237 Powder</p>
<p>No I Holder</p>		

Table 4.1. Loading Plan of Cavity Dosimetry Holders (Cont'd)

Holder and Location	Unshielded Positions 1, 2 (Aluminum Cases)	Shielded Positions 3, 4, 5 (Gadolinium Cases)
<p style="text-align: center;">J</p> <p>11.0° Core Midplane Elevation</p>	<p>1 - B&W RMs Fe Co Co-Al Wire Fe Wire</p> <p>2 - SS Chain #6</p>	<p>3 - B&W RMs Fe Co Nb (ToyoSoda) Nb (MOL) HAFM 3 Be Li</p> <p>4 - B&W RMs Fe Co</p> <p>5 - Co-Al Wire Ni Wire Np-Al Wire U-AL Wire</p>
<p style="text-align: center;">K</p> <p>11.0° Core Midplane Elevation</p>	<p>1 - U of A RM</p> <p>2 - B&W RMs Fe Co SS Chain #7</p>	<p>3 - U of A RM</p> <p>4 - U of A RM</p> <p>5 - B&W RMs Fe Co</p>

Table 4.1. Loading Plan of Cavity Dosimetry Holders (Cont'd)

Holder and Location	Unshielded Positions 1, 2 (Aluminum Cases)	Shielded Positions 3, 4, 5 (Gadolinium Cases)
<p style="text-align: center;">L</p> <p>6° Core Midplane Elevation</p>	<p>1 - HEDL RM B&W RMs Co-Al Wire Fe Wire</p> <p>2 - B&W RMs 2 Fe 2 Co Co-Al Wire Fe Wire</p>	<p>3 - HEDL RM B&W RMs Co-Al Wire Ni Wire Np-Al Wire U-Al Wire</p> <p>4 - B&W RMs Fe Ni Cu Co Co-Al Wire Ni Wire Np Wire U-Al Wire</p> <p>5 - B&W RMs Fe Co</p>
<p style="text-align: center;">N</p> <p>42.5° Core Midplane Elevation</p>	<p>1 - B&W SSTR (33B)</p> <p>2 - B&W RM Fe Co Co-Al Wire Fe Wire</p>	<p>3 - B&W RMs Fe Ni Cu Co</p> <p>4 - Co-Al Wire Ni Wire Np Wire U-Al Wire B&W SSTR (33C)</p> <p>5 - 2 Np-237 Powder</p>
<p>No 0 Holder</p>		

4.1. Loading Plan of Cavity Dosimetry Holders (Cont'd)

Holder and Location	Unshielded Positions 1, 2 (Aluminum Cases)	Shielded Positions 3, 4, 5 (Gadolinium Cases)
<p style="text-align: center;">P</p> <p>26.5° Core Midplane Elevation</p>	<p>1 - 2 Co-Al Wire 2 Fe Wire</p> <p>2 - B&W RMs Fe Co Co-Al Wire Fe Wire</p>	<p>3 - LiF</p> <p>4 - 2 Co-Al Wire 2 Ni Wire 2 Np Wire 2 U-Al Wire</p> <p>5 - U-Al Wire Np Wire Co-Al Wire Ni Wire</p>
<p style="text-align: center;">Q</p> <p>26.5° Core Midplane Elevation</p>	<p>1 - B&W RMs Fe Co</p> <p>2 - B&W RMs Fe Co</p>	<p>3 - B&W RMs Fe Ni Cu Co Nb (ToyoSoda) HAFM 3 Be Li</p> <p>4 - B&W RMs Fe Co</p> <p>5 - HAFM 3 Be Li Nb (MOL) 2 Nb (ToyoSoda)</p>

Table 4.1. Loading Plan of Cavity Dosimetry Holders (Cont'd)

Holder and Location	Unshielded Positions 1, 2 (Aluminum Cases)	Shielded Positions 3, 4, 5 (Gadolinium Cases)
<p style="text-align: center;">R</p> <p>11.5° Seal Plate Elevation</p>	<p>1 - Bechtel RMs Fe Co</p> <p>2 - Bechtel SSTR (B&W-1) B&W SSTR (1B)</p>	<p>3 - LiF</p> <p>4 - Bechtel RMs Fe Ni 3 Cu Co B&W SSTR (1C)</p> <p>5 - Bechtel SSTR (B&W-3) Bechtel SSTR (B&W-2)</p>
<p style="text-align: center;">S</p> <p>11.5° Core Midplane Elevation Source Tube "A"</p>	<p>1 - B&W RMs Fe Co</p> <p>2 - B&W SSTRs (5B, 6B)</p>	<p>3 - R&W RMs Fe Ni Cu Co</p> <p>4 - Nb (ToyoSoda) B&W SSTRs (6C, 5C, B&W-15, B&W-16)</p> <p>5 - MOL RM</p>

<p style="text-align: center;">T</p> <p>11.5° Core Midplane Elevation</p> <p>Source Tube "B"</p>	<p>1 - HEDL RM</p> <p>2 - B&W RMs Fe Co</p>	<p>3 - LiF</p> <p>4 - HEDL RM Bechtel SSTR (B&W-6)</p> <p>5 - HAFM 3 Be 1 Li HAFM 3 Be 1 Li 2 Nb (MOL) 2 ToyoSoda Nb B&W RMs Fe Ni Cu Co</p>
--	---	--

Table 4.1. Loading Plan of Cavity Dosimetry Holders (Cont'd)

Holder and Location	Unshielded Positions 1, 2 (Aluminum Cases)	Shielded Positions 3, 4, 5 (Gadolinium Cases)
<p style="text-align: center;">U</p> <p>11.5° Core Midplane Elevation</p> <p>Source Tube "Connector"</p>		<p>4 - B&W RMs</p> <p>Fe</p> <p>Ni</p> <p>Cu</p> <p>Co</p> <p>B&W SSTR (B&W-7 = 8C)</p>

Notes:

- 1) LiF detector chips are in shielded locations, but are in aluminum cases.
- 2) MOL RMs use aluminum cases with internal Cd shielding.

Key:

- B&W = BWNS supplied dosimetry
- HEDL = Hanford Engineering Development Laboratory supplied dosimetry package
- MOL = Center for the Study of Nuclear Energy, MOL Belgium supplied dosimetry package
- PUD = Paired Uranium Detector
- RM = Radiometric Monitor
- SSTR = Solid State Track Recorder
- HAFM = Helium Accumulative Fluence Monitor
- U of A = University of Arkansas supplied dosimetry package (now property of Arkansas Tech University)
- LiF = Lithium Fluoride detector

Table 4.2. Coordinate Location of Dosimetry

Holder I.D.	Azimuth (deg)	Radial (in)	Axial (in)
11 1/2 Degrees			
A	191.5	114.625"	- 17.459"
R	191.5	114.625"	- 26.147"
B	191.5	115.375"	- 79.959"
C	191.5	115.375"	- 88.647"
D	191.5	115.375"	-133.959"
E	191.5	115.375"	-142.616"
F	191.5	115.375"	-205.366"
G	191.5	115.375"	-214.459"
26 1/2 Degrees			
Q	206.5	119.297"	-206.238"
P	206.5	119.297"	-213.762"
42 1/2 Degrees			
H	222.5	115.982"	-206.238"
N	222.5	115.982"	-213.762"
11 Degrees			
J	349.0	115.375"	-205.428"
K	349.0	115.375"	-214.490"
6 Degrees			
M	6.0	115.185"	-210.603"
L	6.0	115.185"	-219.166"
Permanent (11 1/2°)			
S	191.8	128.812"	-201.625*
T	191.8	128.812"	-220.875*

*Elevation dimensions for the Permanent dosimetry capsules are taken to the center line of the center capsule lid closure bolts for both the upper and lower capsules.

FIGURE 4.1 IS FTI PROPRIETARY

Figure 4.2 General Arrangement of Cavity Dosimetry Benchmark Experiment

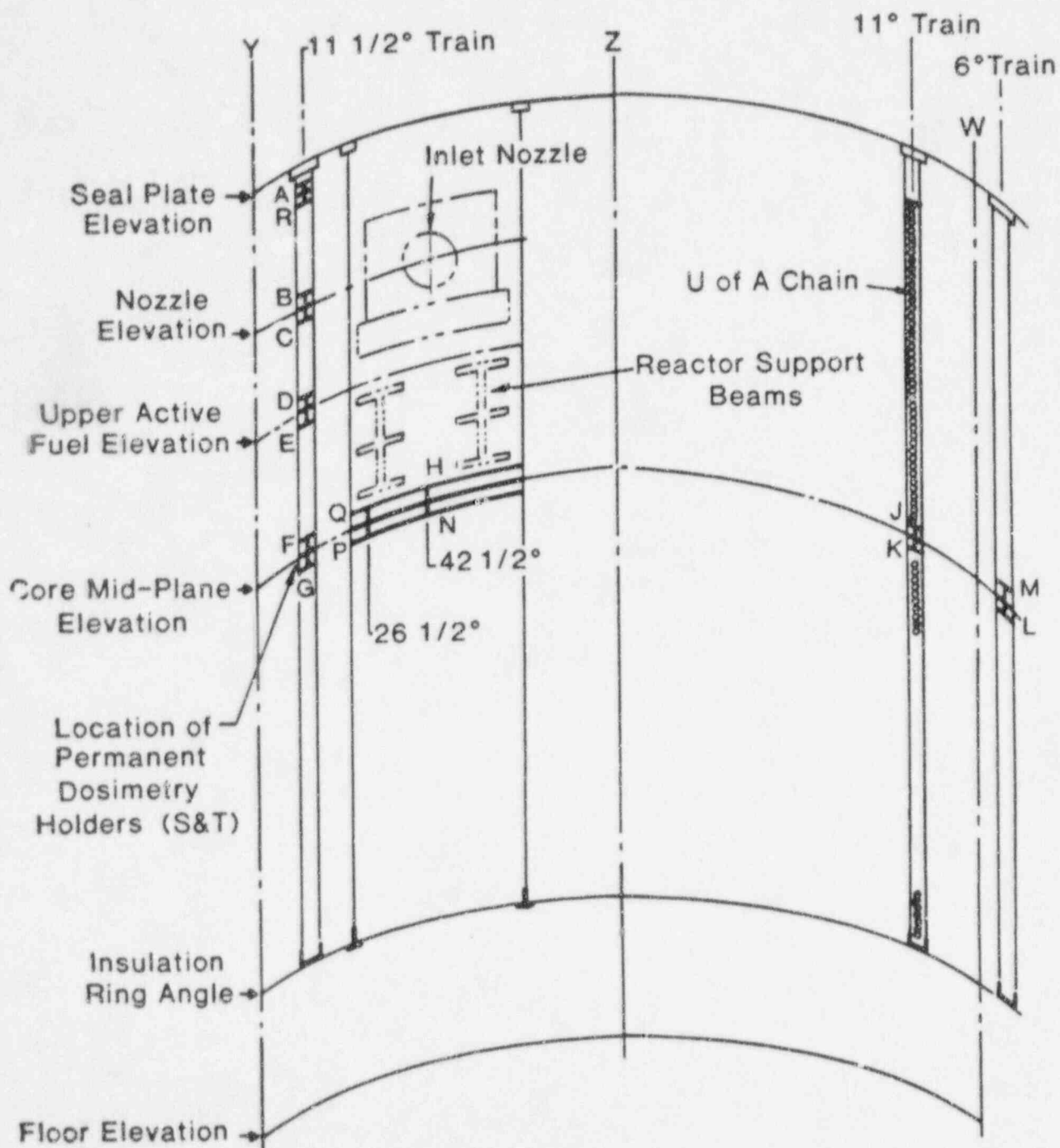


FIGURE 4.3 IS FTI PROPRIETARY

FIGURE 4.4 IS FTI PROPRIETARY

5.0 Measurement Methodology

There were three categories of neutron dosimeters irradiated in the experiment:

1. Radiometric Dosimeters: fissionable, activation, niobium, and stainless-steel chains (Section 5.1),
2. Solid State Track Recorders (Section 5.2), and
3. Helium Accumulation Fluence Monitors (Section 5.3).

For each of these three categories of neutron detectors, the indicated subsection provides a discussion of the measurement techniques, the corrections required to determine specific activity from counting data, and the measurement results.

5.1 Radiometric Dosimeters

The radiometric dosimeters, including stainless steel chains, were analyzed by B&W Nuclear Environmental Services (NES) at its Lynchburg Research Center. The measurement techniques, corrections, and measured results are reported in References 24 and 25. A summary of the measurement techniques, corrections, and results, however, is included in this section.

5.1.1 Fissionable Radiometric Dosimeters (U-235, U-238, Np-237)

Forty-seven fissionable radiometric dosimeters were irradiated in Davis-Besse Cycle 6 at locations described in Section 3 and the capsule.

5.1.1.1 Measurement Techniques

One measurement technique was used for the wires, foils, and vanadium encapsulated oxide wires while another was used for the powder dosimeters. Each wire, foil, and encapsulated dosimeter was washed and dried. Its diameter or thickness was measured with a micrometer and it was weighed on an analytical balance. Each dosimeter was then mounted on a PetriSlide™ with double-sided tape and a preliminary 300 second count was taken on the 31% Princeton Gamma-Tech (PGT) gamma spectrometer to select the best distance from dosimeter to detector to be used in the final count. The target for the final count was 10,000 counts in the photo-peak of interest while keeping the counter dead time below 15%.

The ^{137}Cs 662 keV gamma was counted and analyzed for all of the fissionable radiometric dosimeters. In addition, the ^{233}Pa 312 keV gamma was counted for some ^{237}Np dosimeters, the ^{235}U 186 keV gamma for the ^{235}U dosimeter and the $^{234\text{m}}\text{Pa}$ 1001 keV gamma for some ^{238}U dosimeters. The counting data was taken and processed with a computer-based multichannel analyzer using the shutdown date of January 26, 1990 as the reference date for decay corrections. The detector was calibrated for the foil, wire and encapsulated dosimeters with a NIST-traceable mixed gamma "point source" standard. The source was actually a thin spot a few millimeters in diameter. The mounting of the dosimeters was such that the side of the dosimeter closest to the detector was in the same plane as the standard source. A correction was therefore required in most cases for the fact that the effective distance from the dosimeter to the detector differed slightly from the standard to detector distance. This is discussed below with other corrections.

The data is reported in micro-Curies per gram of target ($\mu\text{Ci/gm}$) where the target is the first named isotope in the designation of each reaction. The fraction of the dosimeter mass that corresponds to the mass of each fissionable isotope was therefore required. It was determined from information on the fraction of the aluminum alloy mass that was ^{238}U or ^{237}Np , the fraction of the oxide mass that was ^{238}U , ^{235}U or ^{237}Np , and the fraction

of the mass of encapsulated dosimeters that was vanadium.

A different measurement technique was used for the fissionable oxide powders. The uranium oxide dosimeters were dissolved in HNO_3 and diluted to 20 mL in a scintillation vial. The neptunium oxide dosimeters were digested in 6N HCl /16N HF with addition of 30% H_2O_2 until dissolved and were also diluted to 20 ml in a scintillation vial. The activity for each was determined by counting the ^{137}Cs 662 keV gamma with the PGT gamma spectrometer and decay correcting to January 26, 1990. A NIST-traceable mixed gamma standard was counted in an identical geometry, therefore, no corrections for geometry or attenuation were required for the dissolved dosimeters. The mass of uranium was determined by inductively coupled plasma atomic emission spectroscopy and the mass of neptunium was determined from the measured ^{233}Pa content using the 312 keV gamma.

5.1.1.2 Corrections

As stated above, the data for the wires, foils and encapsulated wires were corrected for the difference between the effective distance from dosimeter to detector and the standard to detector distance. In the standard correction contained in the NES spread sheets, the dosimeters are partitioned into four slabs parallel to the face of the detector. A correction factor is determined for each slab assuming that the response varies as the reciprocal of the distance to the detector squared. The geometry factor for the dosimeter is then obtained from a weighted average of the slab factors using the cross-sectional area of each slab as the weight.

The dosimeter results are also corrected for self-absorption of the 662 keV gamma used to measure the ^{137}Cs activity. In the standard correction in the NES spread sheets the narrow angle formula by W. R. Dixon²⁶ is used for foils and a formula by Evans and Evans²⁷ is used for cylindrical wires. The equation for foils is

$$I_o = I \frac{\mu t}{1 - e^{-\mu t}} \quad (5.1)$$

where

μ = $\rho \mu_o$ a linear attenuation coefficient, cm^{-1}

ρ = density, gm/cm^3

μ_o = mass attenuation coefficient, cm^2/gm

t = foil thickness, cm

I = measured intensity with self absorption

I_o = corrected intensity

The equation for wires is similar in principle but has many more terms. The correction is a function of the linear attenuation coefficient, the radius of the wire, and the distance from wire to detector. Values for the mass attenuation coefficients were interpolated from the Storm and Israel tables.²⁸ Linear attenuation coefficients for alloys and oxides were obtained from the mass coefficient for each constituent and combined as a mixture.

The corrections for all the fissionable radiometric dosimeters were first made using the standard corrections contained in the NES spread sheets. The results in Reference 24 are based on these corrections. The approximations contained in these corrections are valid when the wire diameter or foil thickness is small and when the distance from the dosimeter to the detector is large. Most of the fissionable radiometric dosimeters, however, did not meet this criteria. For this reason, a Monte Carlo method was used to calculate the correction factors for the fissionable dosimeters except for the thin foil and powders. The foils met the criteria, and the powdered dosimeters did not require corrections.

The Monte Carlo method is the same as used for niobium and described in Section 5.1.3. The code, named NIOBIUM, was used with input appropriate for the 662 keV ^{137}Cs gamma rather than the 16.6 keV X-ray used for niobium in Section 5.1.3. In this code, gammas are started isotropically with a uniform distribution throughout the dosimeter. A hit is recorded for all gammas that both escape the dosimeter and travel in a direction to hit the detector. A sufficient number of histories are used to record at least 10,000 hits at the detector. Three cases were calculated:

1. Source of gammas distributed in actual dosimeter geometry and actual attenuation coefficient.
2. Source of gammas distributed in actual dosimeter geometry and a vanishingly small attenuation coefficient.
3. Source of gammas distributed in point source geometry and with a very small attenuation coefficient.

A total correction factor may be obtained from the ratio of Case 3 to Case 1. The geometry factor is the ratio of Case 2 to Case 3 and the self-absorption factor is the ratio of Case 2 to Case 1. The ratio of the total correction calculated with the Monte Carlo method to the total correction calculated using the standard method is included with the results.

The diameter of each vanadium encapsulated wire was estimated using measured dosimeter mass and vendor supplied data on mass and composition of the encapsulated wire. The Monte Carlo method was used to calculate the geometry and self-absorption factors assuming that the wire was at the center of the dosimeter. In addition, a correction factor of 1.008 was applied to account for the transmission through the vanadium wall. This corresponds to an effective wall thickness of 0.0075 inch.

The concentration of ^{235}U in most of the ^{238}U dosimeters is approximately 12 ppm. The

one exception to this is the uranium aluminum alloy where the concentration is 350 ppm. This level is high enough to require a correction to the uranium alloy data. The K4 location in the cavity contained both a ^{235}U and ^{238}U gadolinium covered dosimeter. A correction factor of 0.9074 was derived from the measured data. Similarly calculated data for ^{235}U and ^{238}U in a surveillance capsule inside the reactor leads to a correction factor of 0.952.

Corrections were also made for photofissions in ^{238}U and ^{237}Np , in both the surveillance capsules and the cavity. Calculated correction factors based on cross sections in the upper three energy gamma groups in the CASK group structure are as follows:

	^{238}U	^{237}Np
Surveillance Capsule	0.950	0.980
Cavity	0.968	0.994

5.1.1.3 Measured Results

The measured activities per gram of target nuclide is listed in Appendix B, (1) Table B-1.1-1 for the ^{238}U radiometric dosimeters, (2) Table B-1.1-2 for the ^{237}Np radiometric dosimeters, and (3) Table B-1.1-3 for the one ^{235}U radiometric dosimeter. The correction factors used for photofissions and ^{235}U and ^{238}U are listed as well as factors to correct the Monte Carlo method of calculating the geometry and self-absorption factors.

5.1.2 Non-Fissionable Radiometric Dosimeters

Two-hundred and forty-three non-fissionable radiometric dosimeters were irradiated in Davis-Besse Cycle 6. In addition, four stainless steel beaded chains were divided into segments and counted as discussed in Section 5.1.4. The distribution by type and general location is given in Table 5.1.2-1.

5.1.2.1 Measurement Techniques

The measurement technique is basically the same as described in Section 5.1.1 for fissionable wires and foils. The dosimeters were washed, dried, measured, weighed, and each dosimeter was mounted on a PetriSlide™ with double-sided tape. A preliminary 300 second count was taken on the 31% PGT gamma spectrometer to select the best distance from dosimeter to detector to be used in the final count. The target for the final count was 10,000 counts in the photopack of interest while keeping the counter dead time below 15%.

The photopeaks used to determine the activity for each dosimeter are listed in Table 5.1.2-2. The detector was calibrated with a NIST-traceable mixed gamma "point source". The dosimeter data was processed with a computer-based multichannel analyzer using the shutdown date of January 26, 1990 as the reference date for decay corrections. The data is reported in micro-Curies per gram of target isotope. The fraction of the dosimeter mass corresponding to the target isotope mass is, therefore, required. This was obtained from the weight fraction of the element in the alloys and/or the weight fraction of the target in the element. The weight fraction for all of the dosimeters is summarized in Table 5.1.2-3. The impurities in the dosimeters were sufficiently low such that they did not affect the target weight.

5.1.2.2 Corrections

Two corrections were made to the non-fissionable radiometric data. One was the geometry correction which accounts for the slight difference in effective distance from the dosimeter to the detector and the distance from standard to detector. The other was the self-absorption correction. The corrections for wires and foils for non-fissionable radiometric dosimeters are identical to the standard corrections for fissionable radiometric wires and foils described in Section 5.1.1.

5.1.2.3 Measured Results

The measured results for the activity per gram of target are listed in Appendix B Tables B-1.2-4 through B-1.2-11. The geometry and self-absorption correction factors are also listed. The conventional treatment of the two factors is such that the uncorrected data is divided by the geometry factor and multiplied by the self-absorption factor to yield the corrected data.

5.1.3 Niobium Dosimeters

Twenty two high purity niobium dosimeters were exposed in the cavity in Davis-Besse during Cycle 6. Twenty of these were near midplane, one was at the upper active fuel elevation and one was at the nozzle elevation. Of the twenty-one which will be compared, four were part of the MOL dosimeters, two were part of the AT4 dosimeters, and fifteen were part of the B&W dosimeters. The fifteen B&W niobium dosimeters include ten low Ta dosimeters obtained from Toyo Soda and five obtained from MOL.

5.1.3.1 Measurement Techniques

SECTIONS 5.1.3.1 AND 5.1.3.2 ARE FTI PROPTIETARY

5.1.3.3 Measured Results

The measured activity of ^{93m}Nb per gram of ^{93}Nb is listed in Appendix B, Table B-1.3-1 for each of the 22 Nb dosimeters. The activity due to fluorescence caused by ^{182}Ta and ^{94}Nb is also listed. In all cases, the correction for fluorescence was very low. This is due to a combination of low tantalum and a long wait time from the end of the irradiation to the time that the dosimeter activities were measured. The correction for ^{94}Nb fluorescence ranged from 0.16% to 0.38% for all dosimeters other than the one in location C4 which was 1.3%. The correction for ^{182}Ta fluorescence was less than 0.1% for all dosimeters except (a) the foil in location K3 which was 3.2%, (b) the wire in K3 which was 0.45%, and (c) the four MOL dosimeters in F5 and S5 which averaged 2.3%.

5.1.4 Stainless Steel Chains

Four B&WOG stainless steel chains located as shown in Figure 4.4 were irradiated

during Cycle 6. The chains consisted of thin wall hollow spherical beads connected together with short wire links. The beads are 0.468 cm in diameter and weigh approximately 0.21 gm per bead with four beads per inch of chain length. The chains extended from near the seal plate to the concrete floor. Samples were cut from the chains and analyzed for both the $^{54}\text{Fe}(n,p)^{54}\text{Mn}$ and $^{59}\text{Co}(n,\gamma)^{60}\text{Co}$ reactions to provide axial flux distribution information. Nine one-inch long chain segments were also loaded in "pill boxes" for comparison with the conventional radiometric dosimeters.

5.1.4.1 Measurement Techniques

The measurement technique for the chain segments was similar to that for the other radiometric dosimeters. However, because of the significant difference in geometry, the corrections were determined in a different way. After cleaning, the chains were cut as required and each measurement segment was weighed and mounted on a PetriSlide™ using a double-sided tape and spiraling the chain segments around the center of the slide. Measurement segments were cut every six inches over the height of the fuel, near the upper concrete lip, and near the nozzle elevation. Otherwise, segments were cut every 12 inches. The measurement segments were two-inches long (eight beads) from 30 inches above the fuel to 36 inches below the fuel and the remainder of the segments were four-inches long (16 beads).

The 834 keV photo-peak from ^{54}Mn was used to analyze the ^{54}Fe reaction and the 1332 keV photopeak from ^{60}Co was used to analyze the $^{59}\text{Co}(n,\gamma)^{60}\text{Co}$ reaction. The detector was calibrated with a NIST traceable mixed gamma "point source" and the data was processed with a computer-based multichannel analyzer using the shutdown date of January 26, 1990 as the reference date for decay corrections.

The fraction of the mass of the chain segments corresponding to ^{54}Fe and to ^{59}Co is

required to express the activity in microcuries per gram of target isotope. Unirradiated samples of the chains were dissolved in HCl/HNO₃ acid and were analyzed by inductively coupled plasma atomic emission spectrometry. The elemental weight fraction was determined to be 0.6693 for Fe and 0.0037 for Co. After combining with the isotopic weight fractions, the fraction of the chain mass that is ⁵⁴Fe was determined to be 0.0382 and the fraction that is ⁵⁹Co is 0.0037.

5.1.4.2 Corrections

Two corrections were made to the chain data. One was a geometric correction which accounts for the difference in effective distance from the chain segment to the detector and the distance from the "point source" standard to the detector. The other was a correction for the absorption within the chain systems of the 834 keV gammas in the ⁵⁴Mn case and the 1332 keV gammas in the ⁶⁰Co case. The standard method of correcting for self-absorption could not be applied to the chain segments because of the difference in geometry from either foils or wires. The standard wire geometric formula, however, gives a good approximation for the geometry factor. In this case, the standard wire formula yields a geometric factor of 0.9402. This is for a diameter of 0.46778 cm and a shelf-to-detector distance of 7.387 cm. The Monte Carlo method was used to confirm that this is also an appropriate value for chain segment at the same shelf distance.

A measured total correction factor was obtained for the ⁶⁰Co measurements.

After the chain segments were analyzed on the PetriSlides™, selected segments were dissolved in 1=1 HCl/HNO₃ acid and diluted to 500 mL in a Marinelli beaker. The ⁶⁰Co activity was then measured with the gamma spectrometer calibrated for the Marinelli geometry using a NIST traceable standard. Since no corrections are required for the dissolved Marinelli geometry case, the total correction factor for the chain segment on the PetriSlide™ could be determined by comparing the two measurements.

The ^{60}Co data are very consistent and yield an average total corrector factor of 1.102 ± 0.009 . The total correction factor is:

$$F_{\text{Total}} = F_A/F_G$$

where F_A is the self-absorption factor and F_G is the geometry factor. Using the geometry factor from above gives the following correction factors for the chain segment ^{60}Co data.

$$F_{\text{TOTAL}} = 1.102$$

$$F_G = .9462$$

$$F_A = 1.036$$

An attempt was made to measure the total correction factor for ^{54}Mn in the same way; however, for some unknown reason, the data was very inconsistent. The correction factors for ^{54}Mn were, therefore, determined from the ^{60}Co data. The geometry factor for ^{54}Mn is the same as for ^{60}Co . The only unknown factor is then the self-absorption factor for ^{54}Mn . This was obtained by estimating the difference in self-absorption for the ^{54}Mn 834 keV gamma versus the ^{60}Co 1332 keV gamma in a chain segment. The linear attenuation coefficient for the two gammas in stainless steel was determined using the NIST program XGAM as:

E	μ
1332 keV	0.408 cm^{-1}
834 keV	0.516 cm^{-1}

An effective foil thickness then determines the ^{60}Co self-absorption factor of 1.036 using the standard foil equation and $\mu = 0.408 \text{ cm}^{-1}$. The same formula yields a self-absorption factor of 1.046 using the same thickness and $\mu = 0.516 \text{ cm}^{-1}$. It was assumed

that the fractional change would be the same for the chain segments, therefore, for ^{54}Mn

$$F_G = 0.9402$$

$$F_A = 1.046$$

$$F_T = 1.113$$

5.1.4.3 Measured Results

The measured ^{54}Mn activities per gram of ^{54}Fe and the ^{60}Co activities per gram of ^{59}Co are listed in Appendix B Tables B-1.4-1 through B-1.4-4. The last part of each sample ID is a distance in inches from the top of each chain hanger to the center of each sample. This coordinate will be designated as Z^1 and will be a positive number. Two other axial coordinates are used. Z is an axial coordinate in inches with origin at the seal plate level. A negative value of Z then indicates a point below the seal plate. The top of each chain hanger was 13.5 inches below the seal plate, therefore,

$$Z = Z^1 - 13.5$$

Y designates another axial coordinate which is the distance in cm above the bottom of the lower grid. The relation between Y and Z is:

$$Y = (295.375 + Z) \times 2.54 \quad 5.3$$

The bottom of the active fuel is at $Z^1 = 268.5$ in. Nominal midplane is at 196.5 in. and top of fuel at 124.5 in. based on 144 in. of fuel height. The actual fuel height is approximately 142.5 in. making the top of the fuel at $Z^1 = 126$ in. and midplane at $Z^1 = 197.25$ in.

Activity measurements for the chain segments irradiated in the "pill boxes" are listed in Table B-1.4-5 of Appendix B.

5.2 Solid State Track Recorders (SSTRs)

Solid State Track Recorders (SSTR) neutron dosimeters were prepared at the Hanford Engineering Development Laboratory (HEDL) and the Westinghouse Science & Technology Center (STC) under contract to the B&W Nuclear Service Company for exposure at Davis Besse Unit 1 during operating cycle 6. A total of eighty-five ultra low-mass fissionable deposits of ^{235}U , ^{239}Pu , ^{237}Np , and ^{238}U with mica SSTRs were assembled into thirty-three dosimetry packets. The as-built information for the dosimeters is contained in References 30 and 31. Following irradiation of the dosimeters in the reactor cavity of Davis-Besse during cycle 6, the dosimeters were retrieved and shipped to Westinghouse STC for analysis.

5.2.1 Measurement Techniques

All 85 SSTRs were etched in 49% HF at 22.0°C for a minimum of one hour. Deposit uniformities were consistent with previous experience in most cases and presented no difficulties for track scanning.

Most SSTRs were scanned with the Westinghouse Automated Track Scanner, but in selected cases some were manually scanned. Ten of the cases occurred when the track density exceeded the capabilities of the automated scanner and a manual estimating procedure was used. In all cases, at least two independent scans were performed and replicate agreement between the two scans was required. The minimum and maximum track counts obtained were 3599 and 7×10^5 , respectively, with 60 of the 85 SSTRs having less than 100,000 tracks.

5.2.2 Measured Results

Table B-2.2-1 in Appendix B provides the measurements in Fissions/Atom for each SSTR for which there were no mass problems. These data were taken from Reference 32. The first column contains the alphanumeric dosimeter holder identifier and the numeric position number. Positions 1 and 2 have no thermal neutron shielding, positions 3 through 5 have a gadolinium covering.

5.3 Helium Accumulation Fluence Monitors (HAFMs)

HAFMs are neutron dosimeters that use the accumulation of helium gas as the measurable quantity that is related to neutron fluence.²⁵ The helium is generated through (n, α) reactions in the target material and remains, unchanged, in the detector material for several years after formation. The amount of helium is measured by high-sensitivity gas mass spectrometry.

Eleven aluminum-wrapped beryllium HAFM packages and eleven individual Al-Li wire HAFMs, were fabricated for the B & W Owners Group at Rockwell and were processed by Rockwell for helium analysis. Each beryllium package contained three beryllium pieces weighing from ~1.5 to 4 mg each. The beryllium is from Rockwell Lot 7. Beryllium purity is 99.99%. Measured boron impurity in the beryllium is 8.9 wt. ppm.

The Al-Li alloy HAFMs were in the form of bare wires, 0.5 mm in diameter and ~6 mm long. The Al-Li alloy came from Rockwell Lot 5 material, which was originally fabricated by the Central Bureau for Nuclear Measurements (CBNM) at Geel, Belgium. The composition of the Al-Li is Al-0.73 \pm 0.01 wt. % Li, with a ⁶Li content of 95.7 \pm 0.1 at. %.

5.3.1 Measurement Techniques

5.3.1.1 Beryllium HAFMs

Following identification by package number, each beryllium package was carefully

unwrapped and the individual beryllium samples removed. Each beryllium sample was then examined under a low power optical microscope to verify sample integrity. In addition, the beryllium samples were weighed to compare their post-irradiation mass with that obtained during sample fabrication at Rockwell. In each case, no significant mass change was observed.

After identification and inspection, two of the individual beryllium HAFMs in each package were prepared for duplicate helium analysis. This preparation involved first etching the sample to remove ~0.05 mm off the surface, followed by weighing to determine the etched sample mass. The purpose of the etching step was to remove surface material which could have been affected by α -recoil either into or out of the samples during irradiation.

Duplicate helium analyses are performed routinely to give an indication of the analysis reproducibility and also to give an indication of the gross helium homogeneity within each sample.

5.3.1.2 Al-Li Alloy HAFMs

As was done for the beryllium samples, the Al-Li wire HAFMs were first etched to remove ~0.05 mm of surface material which could have been affected by α -recoil either into or out of the samples. The Al-Li samples were then subdivided into three approximately equal mass specimens. Two of the specimens were subsequently analyzed for their helium content.

The helium content of each specimen was determined by isotope-dilution mass spectrometry following vaporization of each in a resistance-heated tungsten-wire crucible in one of the mass spectrometer system's high-temperature vacuum furnaces. The absolute amount of ^4He released was measured relative to a known quantity of added ^3He "spike."

The ^3He spikes were obtained by expanding and partitioning a known quantity of gas through a succession of calibrated volumes. The mass spectrometer was calibrated for mass sensitivity during each series of runs by analyzing known mixtures of ^3He and ^4He .

5.3.2 Measured Results

The results of the helium measurements are given in Appendix B Tables B-4.2-1 and B-4.2-2, and are listed as total atoms of helium released, and as helium concentrations in atomic parts per million (10^{-6} atom fraction) or in atomic parts per billion (10^{-9} atom fraction).²⁵ Helium concentrations are relative to the total number of Be or ^6Li atoms in each Be or Al-Li specimen, respectively. Conversion from total helium to helium concentration was based on a calculated number of atoms per gram of 6.682×10^{22} for the beryllium, and 0.06942×10^{22} for the Al-Li alloy.

For the beryllium results in Table B-4.2-1, the concentration values listed in Column 5 have been corrected for small amounts of helium previously measured at Rockwell in unirradiated beryllium material from the same Rockwell lot. These measurements indicated an initial helium concentration level in the beryllium of 0.05 appb. The Column 5 data have also been corrected for helium generation from the small boron impurity (8.9 wt. ppm) in the Lot 7 beryllium. This latter correction was calculated from the helium concentrations measured in the Al-Li HAFMs at the same reactor locations (assuming a $^{10}\text{B}/^6\text{Li}$ thermal neutron cross section ratio of 4.08), and amounted to only ~0.3% of the total helium generation.

Table 5.1.2-1. Non-Fissionable Radiometric Dosimeters

Type	Midplane and Upper Active Fuel	In-Vessel Capsules	Nozzle and Seal Plate Level	Total
Fe	50	8	14	72
Ni	23	8	5	36
Cu	15		11	26
Ti	9		2	11
Ag/Al	7		2	9
Co/Al	27	16	2	45
Co	31		12	43
Sc	1			1
	163	32	48	243

Table 5.1.2-2. Photopeak Analyzed for Each Reaction

Reaction	Gamma Ray
$^{54}\text{Fe}(n,p) ^{54}\text{Mn}$	834 keV
$^{58}\text{Ni}(n,p) ^{58}\text{Co}$	811 keV
$^{63}\text{Cu}(n, \gamma) ^{60}\text{Co}$	1332 keV
$^{46}\text{Ti}(n,p) ^{46}\text{Sc}$	1121 keV
$^{109}\text{Ag}(n, \gamma) ^{110m}\text{Ag}$	658 keV
$^{59}\text{Co}(n, \gamma) ^{60}\text{Co}$	1332 keV

Table 5.1.2-3. Isotopic Fractions and Weight Fractions of Target Nuclides

Dosimeter	Target Nuclide	Isotopic Fraction of Target	Weight Fraction of Target Element
Cobalt	⁵⁹ Co	1.0000	ALL - 1.0000
Cobalt/Aluminum	⁵⁹ Co	1.0000	BWOG - 0.0066 ATU - 0.0054 HEDL - 0.00117 HEDL - 0.00496 MOL - 0.01
Silver/Aluminum	¹⁰⁹ Ag	0.48624	ATU - 0.0465 HEDL - 0.00147
Iron	⁵⁴ Fe	0.057	ALL - 1.0000
Nickel	⁵⁸ Ni	0.6739	ALL - 1.0000
Copper	⁶³ Cu	0.6850	ALL - 1.0000
Scandium	⁴⁵ Sc	1.0000	ALL - 1.0000
Titanium	⁴⁶ Ti	0.0768	ALL - 1.0000
Uranium	²³⁵ U ²³⁸ U ²³⁸ U/Al ²³⁸ U V encap	1.0000 1.0000 1.0000 1.0000	ATU - 0.4431 BWOG - ICP HEDL - 1.0000 BWOG - 0.1032 ATU - 0.39432 MOL - 0.13746 MOL - 0.14475
Neptunium	²³⁷ Np ²³⁷ Np/Al ²³⁷ Np V encap	1.0000 1.0000 1.0000	BWOG - ²³³ Pa BWOG - 0.0144 ATU - 0.11472 ATU - 0.11348 MOL - 0.21316
Niobium	⁹³ Nb	1.0000	ALL - Monte Carlo
Stainless Steel Chains	⁵⁴ Fe ⁵⁹ Co	0.057 1.0000	BWOG - 0.6702 (ICP) BWOG - 0.0037 (ICP)

6.0 Comparison of Measured-To-Calculated Dosimeter Responses

One of the goals of the Cavity Dosimetry Program was to develop a calculation-based methodology which can be used to accurately determine the flux. This methodology has been developed and was outlined in Section 3.0 . This section presents the traditional *M/C* ratios from the benchmark experiment part of the dosimetry program.

6.1 In-Vessel *M/C*s

Two standard unirradiated surveillance capsules were loaded in the Davis - Besse reactor at the 11° azimuthal position, one on top of the other. These two capsules, TMI2-C and TMI2-E, were irradiated for the duration of cycle 6 and removed after shutdown, which occurred on January 26, 1990, following 380.3 effective full power days of operation.

Each capsule contained a set of 24 radiometric wire dosimeters, defined below:

Dosimeter	Quantity (Per Capsule)	Covered (Y/N)
U238	4	Y
Np237	4	Y
Ni	4	Y
Co	4	Y
Fe	4	N
Co	4	N

Following removal, the dosimetry was shipped to the B & W laboratory for removal from the capsule and counting. The measurement procedures previously described (Sections 5.5.1 and 5.1.2) apply for the in-vessel dosimetry as well as the cavity

dosimetry. The measured activities were decay-adjusted to the time of shutdown.

The previously described DOT analysis (Section 3.3) determined the "calculated responses" for all dosimeters, both in-vessel and ex-vessel, corrected for all known biases.

As discussed below, the in-capsule calculated activities were determined in a slightly different way than the ex-vessel calculated activities were determined.

Accurate determination of the flux in the capsule is possible only if the perturbing effects of the capsule wall and the surveillance specimens are properly accounted for. Since it is not possible to properly account for those effects using r, z geometry, the basis for the in-capsule flux and dosimeter response calculations must be the r, θ DOT calculations.

The fluxes calculated by the r, θ DOT analysis are axially averaged fluxes, and thus they must be corrected to determine the flux at the actual axial dosimeter position. To that end, specific axial synthesis factors, A_z , have been derived.

The three - dimensional flux for any in-vessel capsule dosimeter response calculation is then defined as:

$$\phi_g^{3D} = A_z \phi_g^{R\theta}(r, \theta) \quad (6.1)$$

where g is an energy group index, and $\phi_g^{R\theta}(r, \theta)$ is the flux calculated by the two - dimensional DOT r, θ run at the point defined by its cylindrical coordinates r and θ .

The calculated dosimeter response is then given by:

$$C_d = S_d \sum_g R_{d,g} \phi_g^{3D} \quad (6.2)$$

where S_d is the fraction of saturation of dosimeter d for the irradiation period of interest (see Section 3.3.2), and $R_{d,g}$ is the response function for dosimeter d with incident energy in group g .

Table 6-1 shows the average M/C by dosimeter type together with the number of dosimeters for each type, and the root mean square standard deviation from Equation 6.3 .

Table 6-1 In-Vessel Average M/Cs

Dosimeter Type	No. of Dosimeters	M/C	Deviation (%)
Fe 54	8	0.942	4.0
Ni 58	8	0.968	5.1
Np 237 Rm covered	8	1.176	7.2
U 238 RM covered	8	1.099	4.6
Co-Al covered	8	0.767	3.4
Co-Al bare	5	1.059	7.5

6.2 Ex-Vessel M/Cs

Several dosimeters of various types were installed at numerous locations in the Davis - Besse cavity. Each individual dosimeter response was analytically calculated, and compared with its corresponding measured value. The large amount of data can be analyzed in various ways. The following analysis simply compares the M/C averages of the first and second moments by material type and reaction type. The first moment

average of the M/C values is listed in Table 6-2 along with the number of dosimeters for each material - reaction type.

The statistical quality of the various M/C ratios is obtained by calculating the root mean square standard deviation from the mean variance of the second moment.

$$\text{variance} = \frac{\sum_d \left\{ \left(\frac{M}{C} \right)_d - \left(\overline{\frac{M}{C}} \right) \right\}^2}{N_d - 1} \quad (6.3)$$

$$\text{standard deviation} = \sqrt{\text{variance}}$$

The standard deviations are listed in Table 6-3 for each dosimeter type.

Summarizing:

- No location bias is observed.
- There is a strong bias by dosimeter type. Thermal dosimeters have large deviations, Np dosimeters appear to have special problems, and all other dosimeters show consistently good results.
- The statistical quality of non-thermal dosimeters is very good and shows no obvious aberrations.

Table 6-2 Ex-Vessel Average M/C by Type

Dosimeter	Reaction Type	M/C	No. of Dosimeter
-----------	---------------	-------	------------------

Framatome Technologies, Inc.

Fe54	A	0.954	50
Ni58	C	0.947	23
Cu63	T	0.971	15
Ti46	I	0.994	8
Ag109	V	0.612	2
Co59 (Al)	A	0.562	15
Co59	T	0.275	16
	I O N (covered)		
Nb		1.076	21
Be	HAFM	0.961	3
Np237	F	1.406	14
U238	I	1.087	15
U235	S	0.646	1
	S I O N A B L E (covered)		

Table 6-2 Ex-Vessel Average M/C by Type (Continued)

Dosimeter	Reaction Type	M/C	No. of Dosimeter
Ag109	A	0.652	5
Co59 (Al)	C	0.829	12
Co59	T	0.663	15
	I		
	V		
	A		
	T		
	I		
	O		
	N		
	(bare)		

Table 6-3 Measured-to-Calculated Ratios and Standard Deviations for Cavity Dosimetry

Dosimeter	Reaction Type	M/C	# of Dosimeter	Deviation (%)	
Fe54	Activation (covered)	0.954	50	4.3	
Ni58		0.947	23	3.5	
Cu63		"	0.971	15	3.3
Ti46		"	0.994	8	5.7
Ag109		"	0.612	2	1.8
Co59 (Al)		"	0.562	15	8.8
Co59		"	0.275	16	2.7
Nb		1.076	21	5.9	
Be	HAFM	0.961	8	3.4	
Np237	Fissionable (covered)	1.406	14	19.5	
U238		1.087	15	6.6	
U235		"	0.646	1	---
U235	SSTR (bare)	---	5	---	
Pu239		"	---	4	---
Ag109	Activation (bare)	0.652	5	10.0	
Co59 (Al)		0.829	12	13.6	
Co59		"	0.663	15	11.0

7.0 Uncertainty Methodology

SECTION 7 IS FTI PROPRIETARY

8.0 References

1. David B. Matthews, Project Director, Office of Nuclear Reactor Regulation, United States Nuclear Regulatory Commission, "Cavity Dosimetry Program - Oconee Nuclear Station Units 1, 2, and 3", December 5, 1988, letter to H.B. Tucker Vice President, Duke Power Company.
2. Radiation Shielding Information Center (RSIC), Oak Ridge National Laboratory (ORNL), "BUGLE-80: Coupled 47 Neutron, 20 Gamma-Ray, P₃, Cross-Section Library for LWR Shielding Calculations", DLC-075, August, 1980.
3. T.J. Burns et alia, Oak Ridge National Laboratory, "Preliminary Development of an Integrated Approach to the Evaluation of Pressurized Thermal Shock Risk as Applied to the Oconee Unit 1 Nuclear Power Plant", NUREG/CR-3770 (ORNL/TM-9176), May, 1986.
4. D.L. Selby et alia, Oak Ridge National Laboratory, "Pressurized Thermal Shock Evaluation of the Calvert Cliffs Unit 1 Nuclear Power Plant", NUREG/CR-4022 (ORNL/TM-9408), November, 1985.
5. D.L. Selby et alia, Oak Ridge National Laboratory, "Pressurized Thermal Shock Evaluation of the H.B. Robinson Unit 2 Nuclear Power Plant", NUREG/CR-4183 (ORNL/TM-9567), November, 1985.
6. Title 10 of the Code of Federal Regulations (CFR), Part 50, Section 50-61, "Fracture Toughness Requirements for Protection Against Pressurized Thermal Shock Events", 10 CFR 50.61, June 30, 1993.
7. Radiation Shielding Information Center (RSIC), Oak Ridge National Laboratory (ORNL), "BUGLE-93: Coupled 47 Neutron, 20 Gamma-Ray Group Cross Section Library Derived from ENDF/B-VI for LWR Shielding and Pressure Vessel Dosimetry Applications", DLC-175, April, 1994.
8. Office of Nuclear Regulatory Research, "Calculational and Dosimetry Methods For Determining Pressure Vessel Neutron Fluence", Draft Regulatory Guide DG-1025, U.S. Nuclear Regulatory Commission, September, 1993.
9. S.Q. King, et alia, "Pressure Vessel Fluence Analysis for 177-FA Reactors", BAW-1485P, Rev. 1, April, 1988.
10. A.L. Lowe, Jr., K.E. Moore and J.D. Aadland, "Integrated Reactor Vessel Material Surveillance Program", BAW-1543A, Rev. 2, May, 1985.

11. A.L. Lowe, Jr., W.A. Pavinich, W.L. Kadd, J.K. Schmotzer and C.L. Whitmarsh, "Analysis of Capsule RS1-B, Sacramento Municipal Utility District, Rancho Seco Unit 1", BAW-1702, February, 1982.
12. C.L. Whitmarsh, "Pressure Vessel Fluence Analysis For 177-FA Reactors", BAW-1485, June, 1978.
13. H.S. Palme, G.S. Carter and C.L. Whitmarsh, "Reactor Vessel Material Surveillance Program, Compliance With 10 CFR 50, Appendix H, For Oconee Class Reactors", BAW-10100A, February, 1975.
14. G.T. Snyder and L.H. Bohn, "Reactor Vessel Material Surveillance Program", BAW-10006, June, 1969.
15. R.L. Simons, L.S. Kellogg, E.P. Lippincott, W.N. McElroy and D.L. Oberg, "Re-Evaluation Of The Dosimetry For Reactor Pressure Vessel Surveillance Capsules", NUREG/CP-0029, Volume 2, Proceedings of the Fourth ASTM-EURATOM Symposium on Reactor Dosimetry, National Bureau of Standards, Gaithersburg, Maryland, March 22-26, 1982.
16. G.L. Guthrie, "Charpy Trend Curves Based On 177 PWR Data Points", NUREG/CR-3391, HEDL-TME 83-22, Volume 2, Hanford Engineering Development Laboratory, LWR Pressure Vessel Surveillance Dosimetry Improvement Program, Progress Report, April 1983 - June 1983.
17. Office of Nuclear Regulatory Research, "Radiation Embrittlement Of Reactor Vessel Materials", Regulatory Guide 1.99, Revision 2, U.S. Nuclear Regulatory Commission, May, 1988.
18. Radiation Shielding Information Center (RSIC), Oak Ridge National Laboratory, "CASK 40 Group Coupled Neutron and Gamma Ray Cross Section Data", DLC-23.
19. Office of Nuclear Regulatory Research, "Calculational And Dosimetry Methods For Determining Pressure Vessel Neutron Fluence", Draft Regulatory Guide DG-1053, U.S. Nuclear Regulatory Commission, June, 1996.
20. S.Q. King, "The B & W Owners Group Cavity Dosimetry Program", BAW-1875-A, July, 1986.
21. R. Gold (MC²) and W.N. McElroy (CTS), "Written Comments and Recommendations Related to the Review of the B&WOG (B & W Owners

- Group) Davis-Besse Cavity Dosimetry Benchmark Program", October, 1992, FTI Doc. # 38-1210653-00, released May 19, 1995. (See Page 9.)
22. Office of Nuclear Regulatory Research, "Format And Content Of Plant-Specific Pressurized Thermal Shock Safety Analysis Reports For Pressurized Water Reactors", Regulatory Guide 1.154, U.S. Nuclear Regulatory Commission, January, 1987. (See References 3, 4 and 5 for specific results.)
 23. L.A. Hassler, et alia, "DOT4.3, Two Dimensional Discrete Ordinates Transport Code", (B & W Version of RISC/ORNL Code DOT4.3), FTI Doc. # NPD-TM-24, July, 1986.
 24. Jimmy L. Coor, "Analysis of B&W Owner's Group Davis Besse Cavity Dosimetry Benchmark Experiment", Volumes I, II and III, B & W Nuclear Environmental Services, Inc. (NESI), NESI # 93:136112:02, May, 1993, FTI Doc. # 38-1210656-00, released May 30, 1995.
 25. Brian M. Oliver, "Helium Analyses of Al-Li and Beryllium HAFMs", B & W Contract #961-0A060034, Rockwell International Corporation, January 23, 1992, FTI Doc. # 38-1247227-00, released November 15, 1996.
 26. W.R. Dixon, "Self-Absorption Corrections for Larger Gamma Ray Sources", NUCLEONICS, Volume 8, Number 4, Page 69, April, 1951.
 27. R.D. Evans and R.O. Evans, "Studies of Self-Absorption in Gamma-Ray Sources", Reviews of Modern Physics, 20, Pages 305-326, January, 1948.
 28. E. Storm and H.I. Israel, "Photon Cross-Sections from .001 to 1.00 MeV for Elements 1 through 100", Los Alamos Scientific Laboratory, Los Alamos, NM, LA-3753, UC-34, PHYSICS, TID-4500, June, 1967.
 29. T.G. Williamson and A.C. Chubb, "Niobium Foil, Counting and Correction for Niobium X-rays from Trace Isotopes", UVA/532886/NEEP 90/102, Department of Nuclear Engineering and Engineering Physics, University of Virginia, Charlottesville, Virginia, August, 1989, FTI Doc. # 38-1210279-00, released July 22, 1992.
 30. * F.H. Ruddy and J.G. Seidel, "As-Built Data for Westinghouse R&D Supplied Babcock & Wilcox Solid State Track Recorder Neutron Dosimeters", Westinghouse R&D Report 88-2S31-SSTRB-R4, July 28, 1988.
 31. * F.H. Ruddy, "Updated Mass Tables for Babcock & Wilcox Ultra Low-Mass Solid State Track Recorder Fissionable Deposits", Westinghouse R&D Report 88-2S31-

SSTRB-R3, August 24, 1988.

32. * F.H. Ruddy, et alia, "Neutron Dosimetry Results for Solid State Track Recorders Irradiated in the B&WOG Cavity Dosimetry Benchmark Experiment", STC Report 93-2TD1-BWSCN-R1, Westinghouse STC, March, 1993.
33. Jimmy L. Coor, "Uncertainty Assessment And Results of Niobium Analysis for Davis-Besse Cavity Dosimetry Benchmark Experiment", Volumes I, II and III, B & W Nuclear Environmental Services, Inc. (NESI), NESI # 93:136146:001, July, 1993, FTI Doc. # 31-1022946-00, released July 21, 1995.
34. P.N. Randall, "Basis for Revision 2 of the U.S. Nuclear Regulatory Commission's Regulatory Guide 1.99", Radiation Embrittlement of Nuclear Reactor Pressure Vessel Steels: An International Review (Second Volume), ASTM STP 909, American Society for Testing and Materials, Philadelphia, 1986.
35. H.A. Hassan, et alia, "Power Peaking Nuclear Reliability Factors", BAW-10119P-A, February, 1979.
36. A.B. Copsy, et alia, "Statistical Core Design For B & W Designed 177 FA Plants", BAW-10187P-A, March, 1994.
37. W.N. McElroy, "LWR Pressure Vessel Surveillance Dosimetry Improvement Program: PCA Experiments And Blind Test", Hanford Engineering Development Laboratory, NUREG/CR-1861 (HEDL-TME 80-87), July, 1981.

*Only for information, the SSTR results are not qualified measurements.

APPENDIX A IS FTI PROPRIETARY

Appendix B Measured Dosimetry Results

The measured dosimetry results that have been discussed in Section 5 are presented in this appendix.

Table B-1.1-1 ^{238}U (n, f) ^{137}Cs Activities

Location	Form	Measured Activity $\mu\text{Ci/gm}$	Correction Factors			Corrected Measured Activity $\mu\text{Ci/gm}$
			Photofission	U-235	Geom. and Self Abs. ^(a)	
G5	Foil	8.574-03	0.9680	1.000	1.000	8.300-03
K4	V-Encap.	1.190-02	0.9680	1.000	0.7948	9.155-03
F5	V-Encap.	1.060-02	0.9680	1.000	0.9073	9.310-03
S5	V-Encap.	8.274-03	0.9680	1.000	0.9077	7.270-03
H5	Powder	8.402-03	0.9680	1.000	1.000	8.133-03
L4	Powder	8.253-03	0.9680	1.000	1.000	7.989-03
L4	Powder	8.543-03	0.9680	1.000	1.000	8.270-03
L1	Powder	8.998-03	0.9680	1.000	1.000	8.710-03
G5	U/Al	1.096-02	0.9680	0.9074	0.9198	8.855-03
J5	U/Al	1.144-02	0.9680	0.9074	0.9184	9.228-03
M3	U/Al	1.093-02	0.9680	0.9074	0.9168	8.802-03
M4	U/Al	1.167-02	0.9680	0.9074	0.9170	9.400-03
N4	U/Al	1.017-02	0.9680	0.9074	0.9182	8.203-03
P4	U/Al	9.306-03	0.9680	0.9074	0.9158	7.485-03
P4	U/Al	1.026-02	0.9680	0.9074	0.9188	8.280-03
P5	U/Al	9.474-03	0.9680	0.9074	0.9196	7.653-03
CD1	U/Al	3.743	0.9500	0.9520	0.9576	3.242
CD2	U/Al	1.987	0.9500	0.9520	0.9586	1.723
CD3	U/Al	3.052	0.9500	0.9520	0.9573	2.642
CD4	U/Al	2.936	0.9500	0.9520	0.9610	2.552

Table B-1.1-1 (Cont'd) ^{238}U (n, f) ^{137}Cs Activities

Framatome Technologies Inc.

Location	Form	Measured Activity $\mu\text{Ci/gm}$	Correction Factors			Corrected Measured Activity $\mu\text{Ci/gm}$
			Photofission	U-235	Geom. and Self Abs. ^(a)	
ED1	U/AI	2.147	0.9500	0.9520	0.9667	1.877
ED2	U/AI	3.995	0.9500	0.9520	0.9600	3.469
ED3	U/AI	3.081	0.9500	0.9520	0.9595	2.674
ED4	U/AI	3.021	0.9500	0.9520	0.9564	2.613

^(a) Ratio of total correction factor using Monte Carlo method-to-total factor using standard method.

Table B-1.1-2 ²³⁷Np (*n, f*) ¹³⁷Cs Activities

Location	Form	Measured Activity μCi/gm	Correction Factor Photofission	Correction for Geom. & Self Absorp. Factors ^(a)	Corrected Measured Activity μCi/gm
F5	V-Encap.	1.505-01	0.994	0.9527	1.425-01
K4	V-Encap.	1.402-01	0.994	0.9527	1.328-01
S5	V-Encap.	1.196-01	0.994	0.9527	1.133-01
H5	Oxide Powder	1.523-01	0.994	1.000	1.514-01
N5	Oxide Powder	1.714-01	0.994	1.000	1.704-01
N5	Oxide Powder	1.984-01	0.994	1.000	1.972-01
G5	Np/Al Wire	1.620-01	0.994	0.9074	1.461-01
J5	Np/Al Wire	1.414-01	0.994	0.9186	1.291-01
M3	Np/Al Wire	1.629-01	0.994	0.9262	1.500-01
M4	Np/Al Wire	1.666-01	0.994	0.9263	1.534-01
N4	Np/Al Wire	1.356-01	0.994	0.9634	1.299-01
P4	Np/Al Wire	1.494-01	0.994	0.9702	1.441-01
P4	Np/Al Wire	1.473-01	0.994	0.9262	1.356-01
P5	Np/Al Wire	1.520-01	0.994	0.9279	1.402-01

^(a) Ratio of total correction factor using Monte Carlo method-to-total factor using standard method.

Table B-1.1-2 (Cont'd) ^{237}Np (n, f) ^{137}Cs Activities

Location	Form	Measured Activity $\mu\text{Ci/gm}$	Correction Factor Photofission	Correction for Geom. & Self Absorp. Factors ^(a)	Corrected Measured Activity $\mu\text{Ci/gm}$
CD1	Np/Al Wire	2.180+01	0.980	0.9642	2.060+01
CD2	Np/Al Wire	1.247+01	0.980	0.9629	1.177+01
CD3	Np/Al Wire	1.702+01	0.980	0.9617	1.604+01
CD4	Np/Al Wire	1.660+01	0.980	0.9686	1.576+01
ED1	Np/Al Wire	1.319+01	0.980	0.9678	1.251+01
ED2	Np/Al Wire	2.180+01	0.980	0.9649	2.061+01
ED3	Np/Al Wire	1.764+01	0.980	0.9668	1.671+01
ED4	Np/Al Wire	1.455+01	0.980	0.9683	1.381+01

^(a) Ratio of total correction factor using Monte Carlo method-to-total factor using standard method.

Table B-1.1-3 ^{235}U (n, f) ^{137}Cs Activities

Location	Form	Measured Activity $\mu\text{Ci/gm}$	Correction for Geom. and Self Absorp. Factor ^(a)	Corrected Measured Act. $\mu\text{Ci/gm}$
K4	Vanadium Encap.	2.998	0.8896	2.667

^(a) Ratio of total factor using Monte Carlo method-to-total factor using standard method.

Table B-1.2-4 ^{54}Fe (n, p) ^{54}Mn Activities

Location	Form	Foil Thickness or Wire Diam. cm	Post Irrad. Mass gm	Geometry Factor	Self Absorp. Factor	Activity $\mu\text{Ci}/\text{gram}$ Target
A1	Foil	0.0127	0.14325	0.9913	1.0033	6.042-03
A2	Foil	0.0127	0.13813	0.9913	1.0033	6.179-03
A4	Foil	0.0127	0.14265	0.9913	1.0033	7.821-03
A5	Foil	0.0127	0.14175	0.9913	1.0033	8.252-03
B1	Foil	0.0787	0.78719	0.9431	1.0204	5.130-02
B2	Foil	0.0127	0.14115	0.9913	1.0033	5.316-02
B4	Foil	0.1270	1.22253	0.9189	1.0330	5.440-02
B5	Foil	0.0127	0.14058	0.9913	1.0033	5.645-02
C1	Foil	0.0127	0.14097	0.9913	1.0033	8.116-02
C2	Foil	0.0127	0.13646	0.9913	1.0033	7.980-02
C4	Foil	0.0127	0.14345	0.9913	1.0033	7.002-02
C5	Foil	0.0127	0.14171	0.9913	1.0033	6.999-02
D1	Foil	0.0787	0.79610	0.9481	1.0204	8.443-01
D2	Foil	0.0127	0.14241	0.9913	1.0033	8.734-01
D4	Foil	0.0127	0.14036	0.9913	1.0033	9.927-01
D5	Foil	0.1270	1.21763	0.9480	1.0330	9.957-01
E1	Foil	0.0127	0.13976	0.9913	1.0033	1.495+00
E4	Foil	0.0127	0.14265	0.9913	1.0033	1.295+00
E5	Foil	0.0127	0.14042	0.9913	1.0033	1.256+00
F1	Foil	0.0127	0.14339	0.9945	1.0033	2.782+00
F3	Foil	0.0127	0.13879	0.9945	1.0033	2.733+00

Table B-1.2-4 (Cont'd) ^{54}Fe (n, p) ^{54}Mn Activities

Framatome Technologies Inc.

Location	Form	Foil Thickness or Wire Diam. cm	Post Irrad. Mass gm	Geometry Factor	Self Absorp. Factor	Activity $\mu\text{Ci}/\text{gram}$ Target
F5	Foil	0.0100	0.06435	0.9957	1.0026	2.737+00
G1	Foil	0.0787	0.79179	0.9895	1.0204	2.662+00
G2	Foil	0.0127	0.14382	0.9945	1.0033	2.793+00
G5	Foil	0.0787	0.79280	0.9671	1.0204	2.673+00
H1	Foil	0.0127	0.13649	0.9945	1.0033	2.440+00
H4	Foil	0.0127	0.14139	0.9945	1.0033	2.471
J1	Foil	0.0127	0.14065	0.9945	1.0033	2.871
J3	Foil	0.0127	0.14139	0.9945	1.0033	2.828
J4	Foil	0.0127	0.14178	0.9945	1.0033	2.847
K2	Foil	0.0127	0.13949	0.9945	1.0033	2.875
K3	Foil	0.0152	0.11777	0.9935	1.0039	2.744
K5	Foil	0.0127	0.14324	0.9945	1.0033	2.748
M1	Foil	0.0787	0.79210	0.9895	1.0204	2.812
M2	Foil	0.0127	0.14172	0.9945	1.0033	2.951
M2	Foil	0.0127	0.14285	0.9945	1.0033	2.972
M3	Foil	0.0787	0.79605	0.9671	1.0204	2.823
M4	Foil	0.0127	0.13842	0.9945	1.0033	2.921
M5	Foil	0.0127	0.13748	0.9945	1.0033	2.898
N2	Foil	0.0127	0.13930	0.9945	1.0033	2.490
N3	Foil	0.0127	0.14212	0.9945	1.0033	2.505
P2	Foil	0.0127	0.13991	0.9945	1.0033	2.411

Table B-1.2-4 (Cont'd) ^{54}Fe (n, p) ^{54}Mn Activities

Location	Form	Foil Thickness or Wire Diam. cm	Post Irrad. Mass gm	Geometry Factor	Self Absorp Factor	Activity $\mu\text{Ci}/\text{gram Target}$
Q1	Foil	0.0127	0.14314	0.9945	1.0033	2.240
Q2	Foil	0.0127	0.14132	0.9945	1.0033	2.234
Q3	Foil	0.0127	0.14183	0.9945	1.0033	2.308
Q4	Foil	0.0127	0.13992	0.9945	1.0033	2.316
R1	Foil	0.0127	0.13771	0.9913	1.0033	1.439-02
R4	Foil	0.0127	0.14442	0.9913	1.0033	5.967-03
S1	Foil	0.0127	0.14320	0.9945	1.0033	2.168
S3	Foil	0.0127	0.13941	0.9945	1.0033	2.149
S5	Foil	0.0100	0.06403	0.9957	1.0026	2.189
T1	Foil	0.1270	1.23099	0.9831	1.0330	2.013
T2	Foil	0.0127	0.13932	0.9945	1.0033	2.161
T4	Foil	0.1270	1.22934	0.9480	1.0330	2.113
T5	Foil	0.0127	0.14131	0.9945	1.0033	2.065
U4	Foil	0.0127	0.14429	0.9945	1.0033	2.046
G2	Wire	0.1000	0.15818	0.9585	1.0215	2.789
J1	Wire	0.1000	0.16197	0.9585	1.0215	2.895
M1	Wire	0.1000	0.18389	0.9585	1.0215	2.949
M2	Wire	0.1000	0.21186	0.9585	1.0215	2.956
N2	Wire	0.1000	0.18805	0.9585	1.0215	2.582
P1	Wire	0.1000	0.18140	0.9585	1.0215	2.536
P1	Wire	0.1000	0.18563	0.9585	1.0215	2.435

Table B-1.2-4 (Cont'd) $^{54}\text{Fe} (n, p) ^{54}\text{Mn}$ Activities

Location	Form	Foil Thickness or Wire Diam. cm	Post Irrad. Mass gm	Geometry Factor	Self Absorp Factor	Activity μ Ci/gram Target
P2	Wire	0.1000	0.18198	0.9585	1.0215	2.468
CD1	Wire	0.1022	0.15049	0.9965	1.0224	1.151+03
CD2	Wire	0.0991	0.15723	0.9966	1.0218	6.636+02
CD3	Wire	0.1015	0.15161	0.9965	1.0223	9.745+02
CD4	Wire	0.0995	0.15122	0.9966	1.0218	9.676+02
ED1	Wire	0.0991	0.15266	0.9966	1.0218	7.204+02
ED2	Wire	0.0986	0.15217	0.9966	1.0217	1.279+03
ED3	Wire	0.0998	0.14954	0.9966	1.0219	1.002+03
ED4	Wire	0.0991	0.14503	0.9966	1.0218	1.001+03

Table B-1.2-5 ^{58}Ni (n, p) ^{58}Co Activities

Location	Form	Foil Thickness or Wire Diam. cm	Post Irrad. Mass gm	Geometry Factor	Self Absorp Factor	Activity $\mu\text{Ci/gm}$ Target
A5	Foil	0.0254	0.28640	0.9892	1.0078	1.904-02
B4	Foil	0.0254	0.29551	0.9892	1.0078	1.233-01
B5	Foil	0.0254	0.28837	0.9892	1.0078	1.293-01
C4	Foil	0.0254	0.28646	0.9892	1.0078	1.671-01
D4	Foil	0.0254	0.28743	0.9892	1.0078	2.230
D5	Foil	0.0254	0.29485	0.9892	1.0078	2.281
F3	Foil	0.0254	0.28497	0.9966	1.0078	5.934
F5	Foil	0.0100	0.06733	0.9957	1.0030	6.048
G5	Foil	0.0254	0.28600	0.9892	1.0078	5.984
K1	Foil	0.0254	0.28579	0.9892	1.0078	6.179
M3	Foil	0.0254	0.29453	0.9892	1.0078	6.319
M4	Foil	0.0254	0.28607	0.9892	1.0078	6.342
N3	Foil	0.0254	0.28891	0.9892	1.0078	5.400
Q3	Foil	0.0252	0.28534	0.9892	1.0077	5.096
R4	Foil	0.0254	0.28535	0.9892	1.0078	2.277-02
S3	Foil	0.0254	0.28707	0.9892	1.0078	4.749
S5	Foil	0.0100	0.06725	0.9957	1.0030	4.772
T4	Foil	0.0254	0.29587	0.9892	1.0078	4.525
T5	Foil	0.0254	0.28789	0.9892	1.0078	4.566
U4	Foil	0.0252	0.28680	0.9892	1.0077	4.547
G5	Wire	0.1000	0.16340	0.9585	1.0255	5.818

Table B-1.2-5 (Cont'd) ^{58}Ni (n, p) ^{58}Co Activities

Location	Form	Foil Thickness or Wire Diam. cm	Post Irrad. Mass gm	Geometry Factor	Self Absorp Factor	Activity $\mu\text{Ci/gm}$ Target
J5	Wire	0.1000	0.17211	0.9585	1.0255	6.361
M3	Wire	0.1000	0.15196	0.9585	1.0255	6.313
M4	Wire	0.1000	0.16498	0.9585	1.0255	6.349
N4	Wire	0.1000	0.18124	0.9585	1.0255	5.492
P4	Wire	0.1000	0.14984	0.9585	1.0255	5.329
P4	Wire	0.1000	0.15580	0.9585	1.0255	5.376
P5	Wire	0.1000	0.16184	0.9585	1.0255	5.415
CD1	Wire	0.1007	0.13366	0.9965	1.0262	2.417+03
CD2	Wire	0.1002	0.12979	0.9966	1.0261	1.418+03
CD3	Wire	0.1003	0.12543	0.9965	1.0261	2.129+03
CD4	Wire	0.0991	0.11901	0.9966	1.0258	2.087+03
ED1	Wire	0.0991	0.13555	0.9966	1.0258	1.575+03
ED2	Wire	0.1001	0.12927	0.9966	1.0261	2.762+03
ED3	Wire	0.1002	0.12784	0.9965	1.0261	2.138+03
ED4	Wire	0.0992	0.13288	0.9966	1.0258	2.161+03

Table B-1.2-6 ^{63}Cu (n, α) ^{60}Co Activities

Location	Form	Foil Thickness or Wire Diam. cm	Post Irrad. Mass gm	Geometry Factor	Self Absorp Factor	Activity $\mu\text{Ci/gm}$ Target
A5	Foil	0.0254	0.28902	0.9827	1.0058	2.747-05
A5	Foil	0.0254	0.28974	0.9827	1.0058	1.683-05
A5	Foil	0.0254	0.28935	0.9827	1.0058	4.019-05
B5	Foil	0.0254	0.28888	0.9827	1.0058	8.772-05
B5	Foil	0.0254	0.29017	0.9827	1.0058	9.480-05
C4	Foil	0.0254	0.28958	0.9827	1.0058	1.269-04
C4	Foil	0.0254	0.28938	0.9827	1.0058	1.256-04
D4	Foil	0.0254	0.28951	0.9827	1.0058	2.595-03
F3	Foil	0.0254	0.28925	0.9827	1.0058	7.552-03
F5	Foil	0.0100	0.07052	0.9931	1.0023	7.339-03
K3	Foil	0.0254	0.27214	0.9827	1.0058	7.698-03
M4	Foil	0.0254	0.28933	0.9827	1.0058	8.098-03
N3	Foil	0.0254	0.28909	0.9827	1.0058	6.709-03
Q3	Foil	0.0254	0.28951	0.9827	1.0058	6.549-03
R4	Foil	0.0254	0.28938	0.9827	1.0058	5.416-05
R4	Foil	0.0254	0.28933	0.9827	1.0058	2.526-05
R4	Foil	0.0254	0.28937	0.9827	1.0058	2.312-05
S3	Foil	0.0254	0.28922	0.9827	1.0058	5.848-03
S5	Foil	0.0100	0.06988	0.9931	1.0023	5.817-03
T5	Foil	0.0254	0.28950	0.9827	1.0058	5.662-03
U4	Foil	0.0254	0.28947	0.9827	1.0058	5.585-03

Table B-1.2-6 (Cont'd) ^{63}Cu (n, α) ^{60}Co Activities

Framatome Technologies Inc.

Location	Form	Foil Thickness or Wire Diam. cm	Post Irrad. Mass gm	Geometry Factor	Self Absorp. Factor	Activity $\mu\text{Ci/gm}$ Target
B4	Wire	0.0508	0.36395	0.9659	1.0096	8.087-05
D5	Wire	0.0508	0.36293	0.9659	1.0096	2.671-03
G5	Wire	0.0508	0.33822	0.9659	1.0096	7.557-03
M3	Wire	0.0508	0.34589	0.9659	1.0096	7.923-03
T4	Wire	0.0508	0.38800	0.9659	1.0096	5.573-03

Table B-1.2-7 ^{46}Ti (n, p) ^{46}Sc Activities

Location	Form	Foil Thickness cm	Post Irrad. Mass gm	Geometry Factor	Self Absorp. Factor	Activity $\mu\text{Ci/gm}$ Target
B4	Foil	0.0254	0.15712	0.9827	1.0032	1.409-02
B4	Foil	0.0254	0.15750	0.9827	1.0032	1.384-02
D5	Foil	0.0254	0.15703	0.9827	1.0032	3.946-01
D5	Foil	0.0254	0.15763	0.9986	1.0032	3.209-01*
F5	Foil	0.0127	0.04746	0.9913	1.0016	1.053
G5	Foil	0.0254	0.15748	0.9986	1.0032	1.028*
K1	Foil	0.0381	0.03567	0.9742	1.0048	1.062
M3	Foil	0.0254	0.15761	0.9986	1.0032	1.235*
S5	Foil	0.0127	0.04711	0.9913	1.0016	8.186-01
T4	Foil	0.0254	0.15799	0.9986	1.0032	8.835-01*
T4	Foil	0.0254	0.15765	0.9986	1.0032	9.119-01*

* Low Counts: Therefore, high counting statistics error possible.

Table B-1.2-8 ^{109}Ag (n, γ) ^{110m}Ag Activities

Location	Form	Foil Thickness or Wire Diam. cm	Post Irrad. Mass gm	Geometry Factor	Self Absorp. Factor	Activity $\mu\text{Ci/gm}$ Target
B1	Wire Alloy 0.147 wt% Ag	0.0508	0.09931	0.9785	1.0043	1.468+02
B4	Wire Alloy 0.147 wt% Ag	0.0508	0.10515	0.9785	1.0043	1.258+02
D1	Wire Alloy 0.147 wt% Ag	0.0508	0.10112	0.9785	1.0043	3.300+02
G1	Wire Alloy 0.147 wt% Ag	0.0508	0.07823	0.9785	1.0043	5.679+02
G5	Wire Alloy 0.147 wt% Ag	0.0508	0.09304	0.9785	1.0043	4.588+02
M1	Wire Alloy 0.147 wt% Ag	0.0508	0.08967	0.9785	1.0043	6.062+02
M3	Wire Alloy 0.147 wt% Ag	0.0508	0.09431	0.9785	1.0043	4.861+02
T1	Wire Alloy 0.147 wt% Ag	0.0508	0.10820	0.9785	1.0043	5.953+02
K1	Foil Alloy 4.65 wt% Ag	0.0127	0.04139	0.9983	1.0013	6.828+02

Table B-1.2-9 Cobalt/Aluminum ^{59}Co (n, γ) ^{60}Co Activities

Location	Form	Foil Thickness or Wire Diam. cm	Post Irrad. Mass gm	Geometry Factor	Self Absorp. Factor	Activity $\mu\text{Ci/gm}$ Target
B1	Wire 0.117 wt% Co	0.0508	0.10352	0.9785	1.0030	1.126+02
B4	Wire 0.496 wt% Co	0.0508	0.09817	0.9785	1.0030	6.187+01
D1	Wire 0.117 wt% Co	0.0508	0.10730	0.9785	1.0030	2.605+02
D5	Wire 0.496 wt% Co	0.0508	0.09804	0.9785	1.0030	1.452+02
G1	Wire 0.117 wt% Co	0.0508	0.08711	0.9785	1.0030	4.727+02
G2	Wire 0.66 wt% Co	0.0762	0.01562	0.9681	1.0045	4.652+02
G5	Wire 0.117 wt% Co	0.0508	0.10295	0.9785	1.0030	2.034+02
G5	Wire 0.66 wt% Co	0.0762	0.01848	0.9681	1.0045	1.957+02
J1	Wire 0.66 wt% Co	0.0762	0.01558	0.9681	1.0045	5.262+02
J5	Wire 0.66 wt% Co	0.0762	0.01950	0.9681	1.0045	2.076+02
M1	Wire 0.117 wt% Co	0.0508	0.10272	0.9785	1.0030	5.278+02
M1	Wire 0.66 wt% Co	0.0762	0.01529	0.9681	1.0045	5.218+02
M2	Wire 0.66 wt% Co	0.0762	0.01631	0.9681	1.0045	5.082+02

Table B-1.2-9 (Cont'd) Cobalt/Aluminum ^{59}Co (n, γ) ^{60}Co Activities

Framatome Technologies Inc.

Location	Form	Foil Thickness or Wire Diam. cm	Post Irrad. Mass gm	Geometry Factor	Self Absorp. Factor	Activity $\mu\text{Ci/gm}$ Target
M3	Wire 0.117 wt% Co	0.0508	0.10284	0.9785	1.0030	2.093+02
M3	Wire 0.66 wt% Co	0.0762	0.01800	0.9681	1.0045	2.076+02
M4	Wire 0.66 wt% Co	0.0762	0.01932	0.9681	1.0045	1.998+02
N2	Wire 0.66 wt% Co	0.0762	0.01640	0.9681	1.0045	4.450+02
N4	Wire 0.66 wt% Co	0.0762	0.01877	0.9681	1.0045	1.956+02
P1	Wire 0.66 wt% Co	0.0762	0.01594	0.9681	1.0045	4.009+02
P1	Wire 0.66 wt% Co	0.0762	0.01524	0.9681	1.0045	3.993+02
P2	Wire 0.66 wt% Co	0.0762	0.01557	0.9681	1.0045	4.024+02
P4	Wire 0.66 wt% Co	0.0762	0.01792	0.9681	1.0045	1.849+02
P4	Wire 0.66 wt% Co	0.0762	0.01803	0.9681	1.0045	1.889+02
P5	Wire 0.66 wt% Co	0.0762	0.01838	0.9681	1.0045	1.889+02
T1	Wire 0.496 wt% Co	0.0508	0.10491	0.9785	1.0030	5.884+02
T4	Wire 0.496 wt% Co	0.0508	0.10682	0.9785	1.0030	2.250+02

Table B-1.2-9 (Cont'd) Cobalt/Aluminum ^{59}Co (n, γ) ^{60}Co Activities

Location	Form	Foil Thickness or Wire Diam. cm	Post Irrad. Mass gm	Geometry Factor	Self Absorp. Factor	Activity $\mu\text{Ci/gm}$ Target
F5	Foil 1.0 wt% Co	0.0100	0.02263	0.9957	1.0007	2.798+02
K3	Foil 0.54 wt% Co	0.0127	0.04395	0.9945	1.0009	2.029+02
S5	Foil 1.0 wt% Co	0.0100	0.02270	0.9957	1.0007	2.803+02
CD1	Bare Wire 0.66 wt% Co	0.0759	0.01674	0.9974	1.0046	1.972+05
CD2	Bare Wire 0.66 wt% Co	0.0765	0.01602	0.9974	1.0047	1.014+05
CD3	Bare Wire 0.66 wt% Co	0.0781	0.01544	0.9673	1.0046	3.985+01
CD4	Bare Wire 0.66 wt% Co	0.0759	0.01516	0.9974	1.0046	1.510+05
ED1	Bare Wire 0.66 wt% Co	0.0759	0.01538	0.9682	1.0045	2.407+01
ED2	Bare Wire 0.66 wt% Co	0.0759	0.01639	0.9974	1.0046	1.928+05
ED3	Bare Wire 0.66 wt% Co	0.0759	0.01634	0.9682	1.0045	3.653+01

Table B-1.2-9 (Cont'd) Cobalt/Aluminum ^{59}Co (n, γ) ^{60}Co Activities

Location	Form	Foil Thickness or Wire Diam. cm	Post Irrad. Mass gm	Geometry Factor	Self Absorp Factor	Activity $\mu\text{Ci/gm}$ Target
ED4	Bare Wire 0.66 wt% Co	0.0762	0.01545	0.9974	1.0047	1.535+05
CD1	Shielded Wire 0.66 wt% Co	0.0758	0.01905	0.9974	1.0046	3.956+04
CD2	Shielded Wire 0.66 wt% Co	0.0764	0.02026	0.9974	1.0047	1.981+04
CD3	Shielded Wire 0.66 wt% Co	0.0743	0.01911	0.9974	1.0046	2.645+04
CD4	Shielded Wire 0.66 wt% Co	0.0752	0.01982	0.9974	1.0046	2.603+04
ED1	Shielded Wire 0.66 wt% Co	0.0747	0.01881	0.9974	1.0046	1.902+04
ED2	Shielded Wire 0.66 wt% Co	0.0745	0.01894	0.9974	1.0046	3.663+04
ED3	Shielded Wire 0.66 wt% Co	0.0759	0.02001	0.9974	1.0046	2.636+04
ED4	Shielded Wire 0.66 wt% Co	0.0773	0.01900	0.9973	1.0047	2.676+04

Table B-1.2-10 Cobalt Wires ^{59}Co (n, γ) ^{60}Co Activities

Location	Wire Diameter cm	Post Irrad. Mass gm	Geometry Factor	Self Absorp. Factor	Activity $\mu\text{ci/gm}$ Target
A1	0.0381	0.01592	0.9949	1.0073	2.381+01
A2	0.0381	0.01557	0.9949	1.0073	2.447+01
A4	0.0381	0.01564	0.9949	1.0073	7.186
A5	0.381	0.01515	0.9838	1.0073	8.083
B2	0.0381	0.01068	0.9978	1.0073	8.926+01
B5	0.0381	0.01052	0.9838	1.0073	3.082+01
C1	0.0381	0.01055	0.9978	1.0073	1.113+02
C2	0.0381	0.01055	0.9978	1.0073	1.102+02
C4	0.0381	0.01045	0.9838	1.0073	3.131+01
C5	0.0381	0.01040	0.9949	1.0073	2.938+01
D2	0.0381	0.00529	0.9978	1.0073	2.132+02
D4	0.0381	0.00501	0.9838	1.0073	6.570+01
E1	0.0381	0.00552	0.9978	1.0073	2.504+02
E4	0.0381	0.00511	0.9949	1.0073	6.814+01
E5	0.0381	0.00517	0.9949	1.0073	7.027+01
F1	0.0381	0.00493	0.9978	1.0073	3.854+02
F3	0.0381	0.00557	0.9949	1.0073	1.045+02
G2	0.0381	0.00505	0.9978	1.0073	3.862+02
H1	0.0381	0.00533	0.9978	1.0073	3.578+02
H4	0.0381	0.00497	0.9978	1.0073	1.038+02
J1	0.0381	0.00555	0.9978	1.0073	4.518+02

Table B-1.2-10 (Cont'd) Cobalt Wires ^{59}Co (n, γ) ^{60}Co Activities

Location	Wire Diameter cm	Post Irrad. Mass gm	Geometry Factor	Self Absorp. Factor	Activity $\mu\text{Ci/gm}$ Target
J3	0.0381	0.00522	0.9978	1.0073	1.133+02
J4	0.00381	0.00504	0.9978	1.0073	1.112+02
K2	0.0381	0.00520	0.9978	1.0073	4.409+02
K5	0.0381	0.00507	0.9978	1.0073	1.109+02
M2	0.0381	0.00539	0.9978	1.0073	4.413+02
M2	0.0381	0.00515	0.9978	1.0073	4.444+02
M4	0.0381	0.00558	0.9949	1.0073	1.086+02
M5	0.0381	0.00531	0.9978	1.0073	1.137+02
N2	0.0381	0.00528	0.9978	1.0073	3.713+02
N3	0.0381	0.00514	0.9949	1.0073	1.084+02
P2	0.0381	0.00496	0.9978	1.0073	3.305+02
Q1	0.0381	0.00482	0.9978	1.0073	3.056+02
Q2	0.0381	0.00497	0.9978	1.0073	3.022+02
Q3	0.0381	0.00458	0.9949	1.0073	9.959+01
Q4	0.0381	0.00507	0.9978	1.0073	9.894+01
R1	0.0381	0.01583	0.9978	1.0073	4.330+01
R4	0.0381	0.01589	0.9949	1.0073	9.545
S1	0.0381	0.00476	0.9978	1.0073	4.477+02
S3	0.0381	0.00549	0.9949	1.0073	1.058+02
T2	0.0381	0.00498	0.9978	1.0073	4.229+02
T5	0.0381	0.00551	0.9949	1.0073	1.074+02
U4	0.0381	0.00502	0.9949	1.0073	1.088+02

Table B-1.2-11 ^{45}Sc (n, γ) ^{46}Sc Activities

Location	Form	Foil Thickness cm	Post Irrad. Mass gm	Geometry Factor	Self Absorp. Factor	Activity $\mu\text{Ci/gm}$ Target
K3	Foil	0.0152	0.01198	0.9991	1.0014	3.304+02

Table B-1.3-1 ^{93}Nb (n, n') $^{93\text{m}}\text{Nb}$ Activities

Location	Form	Niobium Source	Total Activity $\mu\text{Ci/gm}$ Target	Activity From ^{182}Ta Fluorescence $\mu\text{Ci/gm}$ Target	Activity From ^{94}Nb Fluorescence $\mu\text{Ci/gm}$ Target	Corrected Activity $\mu\text{Ci/gm}$ Target
C4	Foil	Toyo Soda	3.332-02	-----	4.412-04	3.288-02
E4	Foil	Toyo Soda	3.112-01	1.311-04	1.146-03	3.099-01
F3	Foil	MOL	5.752-01	-----	9.925-04	5.741-01
F3	Foil	Toyo Soda	5.917-01	2.120-04	1.821-03	5.897-01
H4	Foil	Toyo Soda	5.256-01	-----	1.817-03	5.238-01
J3	Foil	Toyo Soda	6.045-01	-----	1.841-03	6.027-01
K3	Foil	ATU	5.889-01	1.869-02	1.832-03	5.684-01
Q3	Foil	Toyo Soda	5.219-01	-----	1.763-03	5.201-01
Q5	Foil	MOL	5.364-01	-----	1.010-03	5.354-01
Q5	Foil	Toyo Soda	5.106-01	2.448-04	1.634-03	5.087-01
Q5	Foil	Toyo Soda	5.255-01	00000	1.663-03	5.239-01
S4	Foil	Toyo Soda	4.379-01	-----	1.658-03	4.361-01
T5	Foil	Toyo Soda	4.921-01	1.694-04	1.598-03	4.903-01
T5	Foil	Toyo Soda	4.488-01	-----	1.583-03	4.472-01

Table B-1.3-1 (Cont'd) ^{93}Nb (n, n') ^{93m}Nb Activities

Location	Form	Niobium Source	Total Activity $\mu\text{Ci/gm}$ Target	Activity From ^{182}Ta Fluorescence $\mu\text{Ci/gm}$ Target	Activity From ^{94}Nb Fluorescence $\mu\text{Ci/gm}$ Target	Corrected Activity $\mu\text{Ci/gm}$ Target
T5	Foil	MOL	4.638-01	-----	7.993-04	4.630-01
T5	Foil	MOL	4.653-01	-----	8.947-04	4.644-01
J3	Foil	MOL	6.128-01	-----	1.007-03	6.118-01
F5	Foil	MOL	6.009-01	1.342-02	1.122-03	5.864-01
F5	Foil	MOL	6.130-01	1.288-02	1.110-03	5.990-01
S5	Foil	MOL	4.882-01	1.200-02	1.040-03	4.751-01
S5	Foil	MOL	4.780-01	1.188-02	1.049-03	4.651-01
K3	Wire	ATU	5.457-01	2.474-03	1.620-03	5.416-01

Table B-1.4-1 ⁵⁴Mn and ⁶⁰Co Activities for Chain in Octant WX

Sample ID	$\mu\text{Ci/gm Target Fe-54}$	$\mu\text{Ci/gm Target Co-59}$
CHN-WX3-1-4.5	Not Measured	Not Measured
CHN-WX3-2-10.5	Not Measured	Not Measured
CHNWX3-3-16.5	Not Measured	Not Measured
CHN-WX3-4-22.5	3.672E-02	7.125E+01
CHN-WX3-5-34.5	4.135E-02	4.898E+01
CHN-WX3-6-46.5	5.305E-02	5.547E+01
CHN-WX3-7-58.5	8.251E-02	6.722E+01
CHN-WX3-8-64.5	8.786E-02	7.402E+01
CHN-WX3-9-70.5	1.023E-01	8.042E+01
CHN-WX3-10-76.5	1.569E-01	8.838E+01
CHN-WX3-11-82.5	1.822E-01	9.824E+01
CHN-WX3-12-94.5	3.317E-01	1.263E+02
CHN-WX3-13-106.5	5.643E-01	1.470E+02
CHN-WX3-14-118.5	9.398E-01	1.787E+02
CHN-WX3-15-124.5	1.089E+00	1.959E+02
CHN-WX3-16-130.5	1.315E+00	2.149E+02
CHN-WX3-17-136.5	1.531E+00	2.302E+02
CHN-WX3-18-142.5	1.661E+00	2.432E+02
CHN-WX3-19-148.5	1.895E+00	2.501E+02
CHN-WX3-20-154.5	1.990E+00	2.599E+02
CHN-WX3-21-160.5	2.057E+00	2.761E+02
CHN-WX3-22-166.5	2.157E+00	2.909E+02

Table B-1.4-1 (Cont'd) ⁵⁴Mn and ⁶⁰Co Activities for Chain in Octant WX

Sample ID	$\mu\text{Ci/gm Target Fe-54}$	$\mu\text{Ci/gm Target Co-59}$
CHN-WX3-23-172.5	2.222E+00	3.049E+02
CHN-WX3-24-178.5	2.256E+00	3.243E+02
CHN-WX3-25-184.5	2.361E+00	3.191E+02
CHN-WX3-26-190.5	2.284E+00	3.178E+02
CHN-WX3-27-196.5	2.355E+00	3.289E+02
CHN-WX3-28-202.5	2.279E+00	3.339E+02
CHN-WX3-29-208.5	2.484E+00	3.379E+02
CHN-WX3-30-214.5	2.264E+00	3.241E+02
CHN-WX3-31-220.5	2.256E+00	3.016E+02
CHN-WX3-32-226.5	2.212E+00	2.860+02
CHN-WX3-33-232.5	2.058E+00	2.712E+02
CHN-WX3-34-238.5	1.934E+00	2.659E+02
CHN-WX3-35-244.5	1.933E+00	2.582E+02
CHN-WX3-36-250.5	1.675E+00	2.470E+02
CHN-WX3-37-256.5	1.512E+00	2.337E+02
CHN-WX3-38-262.5	1.280E+00	2.192E+02
CHN-WX3-39-268.5	1.082E+00	2.028E+02
CHN-WX3-40-280.5	7.149E-01	1.931E+02
CHN-WX3-41-292.5	4.431E-01	1.750E+02
CHN-WX3-42-304.5	2.811E-01	1.529E+02
CHN-WX3-43-316.5	2.067E-01	1.364E+02
CHN-WX3-44-328.5	1.477E-01	1.188E+02

Table B-1.4-1 (Cont'd) ^{54}Mn and ^{60}Co Activities for Chain in Octant WX

Sample ID	$\mu\text{Ci/gm Target Fe-54}$	$\mu\text{Ci/gm Target Co-59}$
-----------	--------------------------------	--------------------------------

CHN-WX3-45-340.5	1.154E-01	1.073E+02
CHN-WX3-46-352.5	9.559E-02	9.852E+01
CHN-WX3-47-364.5	8.357E-02	9.186E+01
CHN-WX3-48-376.5	6.267E-02	8.574E+01
CHN-WX3-49-388.5	4.402E-02	8.265E+01
CHN-WX3-50-400.5	4.107E-02	7.940E+01
CHN-WX3-51-412.5	3.817E-02	7.749E+01
CHN-WX3-52-424.5	4.622E-02	7.608E+01
CHN-WX3-53-436.5	2.060E-02	7.603E+01
CHN-WX3-54-448.5	Not Detected	7.629E+01
CHN-WX3-55-460.5	Not Measured	Not Measured
CHN-WX3-56-472.5	Not Measured	Not Measured

Table B-1.4-2 ⁵⁴Mn and ⁶⁰Co Activities for Chain in Octant XY

Sample ID	$\mu\text{Ci/gm Target Fe-54}$	$\mu\text{Ci/gm Target Co-59}$
CHN-XY4-1-4.5	Not Measured	Not Measured
CHN-XY4-2-10.5	Not Measured	Not Measured
CHN-XY4-3-16.5	Not Measured	Not Measured
CHN-XY4-4-22.5	Not Detected	4.064E+01
CHN-XY4-5-34.5	2.418E-02	2.938E+01
CHN-XY4-6-46.5	4.218E-02	3.374E+01
CHN-XY4-7-58.5	6.203E-02	4.373E+01
CHN-XY4-8-64.5	5.662E-02	5.065E+01
CHN-XY4-9-70.5	1.014E-01	6.088E+01
CHN-XY4-10-76.5	1.061E-01	7.178E+01
CHN-XY4-11-82.5	1.468E-01	8.515E+01
CHN-XY4-12-94.5	2.701E-01	1.163E+02
CHN-XY4-13-106.5	4.531E-01	1.446E+02
CHN-XY4-14-118.5	8.095E-01	1.743E+02
CHN-XY4-15-124.5	1.008E+00	1.936E+02
CHN-XY4-16-130.5	1.196E+00	2.103E+02
CHN-XY4-17-136.5	1.443E+00	2.264E+02
CHN-XY4-18-142.5	1.607E+00	2.370E+02
CHN-XY4-19-148.5	1.690E+00	2.429E+02
CHN-XY4-20-154.5	1.914E+00	2.451E+02
CHN-XY4-21-160.5	1.999E+00	2.454E+02
CHN-XY4-22-166.5	2.127E+00	2.347E+02

Table B-1.4-2 (Cont'd) ⁵⁴Mn and ⁶⁰Co Activities for Chain in Octant XY

Sample Id	$\mu\text{Ci/gm Target Fe-54}$	$\mu\text{Ci/gm Target Co-59}$
CHN-XY4-23-172.5	2.136E+00	2.398E+02
CHN-XY4-24-178.5	2.204E+00	2.473E+02
CHN-XY4-25-184.5	2.243E+00	2.482E+02
CHN-XY4-26-190.5	2.245E+00	2.468E+02
CHN-XY4-27-196.5	2.326E+00	2.516E+02
CHN-XY4-28-202.5	2.396E+00	2.517E+02
CHN-XY4-29-208.5	2.304E+00	2.490E+02
CHN-XY4-30-214.5	2.294E+00	2.462E+02
CHN-XY4-31-220.5	2.183E+00	2.440E+02
CHN-XY4-32-226.5	2.185E+00	2.397E+02
CHN-XY4-33-232.5	2.050E+00	2.529E+02
CHN-XY4-34-238.5	1.892E+00	2.595E+02
CHN-XY4-35-244.5	1.793E+00	2.590E+02
CHN-XY4-36-250.5	1.615E+00	2.529E+02
CHN-XY4-37-256.5	1.408E+00	2.426E+02
CHN-XY4-38-262.5	1.245E+00	2.280E+02
CHN-XY4-39-268.5	1.017E+00	2.115E+02
CHN-XY4-40-280.5	7.001E-01	1.953E+02
CHN-CY4-41-292.5	4.322E-01	1.752E+02
CHN-XY4-42-304.5	Not Measured	Not Detected
CHN-XY4-43-316.5	1.878E-01	1.316E+02
CHN-XY4-44-328.5	1.285E-01	1.148E+02

Table B-1.4-2 (Cont'd) ^{54}Mn and ^{60}Co Activities for Chain in Octant XY

Sample ID	$\mu\text{Ci/gm Target Fe-54}$	$\mu\text{Ci/gm Target Co-59}$
-----------	--------------------------------	--------------------------------

CHN-XY4-45-340.5	1.114E-01	1.026E+02
CHN-XY4-46-352.5	8.277E-02	9.324E+01
CHN-XY4-47-364.5	1.245E-02	8.536E+01
CHN-XY4-48-376.5	4.680E-02	7.980E+01
CHN-XY4-49-388.5	5.997E-02	7.509E+01
CHN-XY4-50-400.5	4.289E-02	6.847E+01
CHN-XY4-51-412.5	Not Detected	6.299E+01
CHN-XY4-52-424.5	3.312E-02	6.115E+01
CHN-XY4-53-436.5	Not Detected	6.083E+01
CHN-XY4-54-448.5	2.643E-02	6.105E+01
CHN-XY4-55-460.5	Not Measured	Not Measured
CHN-XY4-56-472.5	Not Measured	Not Measured

Table B-1.4-3 ⁵⁴Mn and ⁶⁰Co Activities for Chain in Octant YZ

Sample ID	$\mu\text{Ci/gm Target Fe-54}$	$\mu\text{Ci/gm Target Co-59}$
CHN-YZ1-1-4.5	Not Detected	3.675E+00
CHN-YZ1-2-10.5	Not Detected	1.417E+01
CHN-YZ1-3-16.5	9.152E-03	4.059E+01
CHN-YZ1-4-22.5	2.093E-02	6.655E+01
CHN-YZ1-5-34.5	3.452E-02	4.572E+01
CHN-YZ1-6-46.5	3.728E-02	5.002E+01
CHN-YZ1-7-58.5	6.686E-02	5.936E+01
CHN-YZ1-8-64.5	7.180E-02	6.373E+01
CHN-YZ1-9-70.5	8.069E-02	7.104E+01
CHN-YZ1-10-76.5	1.172E-01	7.871E+01
CHN-YZ1-11-82.5	1.486E-01	8.683E+01
CHN-YZ1-12-94.5	2.435E-01	1.092E+02
CHN-YZ1-13-106.5	4.304E-01	1.357E+02
CHN-YZ1-14-118.5	7.159E-01	1.650E+02
CHN-YZ1-15-124.5	8.683E-01	1.864E+02
CHN-YZ1-16-130.5	1.021E+00	2.036E+02
CHN-YZ1-17-136.5	1.183E+00	2.144E+02
CHN-YZ1-18-142.5	1.324E+00	2.294E+02
CHN-YZ1-19-148.5	1.043E+00	2.345E+02
CHN-YZ1-20-154.5	1.140E+00	2.565E+02
CHN-YZ1-21-160.5	1.247E+00	2.762E+02
CHN-YZ1-22-166.5	1.204E+00	2.764E+02

Table B-1.4-3 (Cont'd) ⁵⁴Mn and ⁶⁰Co Activities for Chain in Octant YZ

Sample ID	$\mu\text{Ci/gm Target Fe-54}$	$\mu\text{Ci/gm Target Co-59}$
CHN-YZ1-23-172.5	1.399E+00	3.042E+02
CHN-YZ1-24-178.5	1.402E+00	3.154E+02
CHN-YZ1-25-184.5	1.310E+00	2.955E+02
CHN-YZ1-26-190.5	1.450E+00	2.737E+02
CHN-YZ1-27-196.5	1.442E+00	2.868E+02
CHN-YZ1-28-202.5	1.362E+00	2.875E+02
CHN-YZ1-29-208.5	1.463E+00	3.025E+02
CHN-YZ1-30-214.5	1.508E+00	2.996E+02
CHN-YZ1-31-220.5	1.342E+00	2.822E+02
CHN-YZ1-32-226.5	1.416E+00	2.710E+02
CHN-YZ1-33-232.5	1.398E+00	2.561E+02
CHN-YZ1-34-238.5	1.327E+00	2.333E+02
CHN-YZ1-35-244.5	1.360E+00	2.328E+02
CHN-YZ1-36-250.5	1.491E+00	2.408E+02
CHN-YZ1-37-256.5	1.410E+00	2.412E+02
CHN-YZ1-38-262.5	1.270E+00	2.295E+02
CHN-YZ1-39-268.5	1.105E+00	2.161E+02
CHN-YZ1-40-280.5	7.383E-01	1.929E+02
CHN-YZ1-41-292.5	4.995E-01	1.725E+02
CHN-YZ1-42-304.5	3.278E-01	1.516E+02
CHN-YZ1-43-316.5	2.095E-01	1.330E+02
CHN-YZ1-44-328.5	1.650E-01	1.150E+02

Table B-1.4-3 (Cont'd) ^{54}Mn and ^{60}Co Activities for Chain in Octant YZ

Sample ID	$\mu\text{Ci/gm Target Fe-54}$	$\mu\text{Ci/gm Target Co-59}$
-----------	--------------------------------	--------------------------------

CHN-YZ1-45-340.5	1.22E-01	1.011E+02
CHN-YZ1-46-352.5	7.634E-02	9.250E+01
CHN-YZ1-47-364.5	7.326E-02	8.527E+01
CHN-YZ1-48-376.5	5.037E-02	7.879E+01
CHN-YZ1-49-388.5	4.719E-02	7.410E+01
CHN-YZ1-50-400.5	2.977E-02	7.022E+01
CHN-YZ1-51-412.5	Not Detected	6.791E+01
CHN-YZ1-52-424.5	3.099E-02	6.568E+01
CHN-YZ1-53-436.5	Not Detected	6.419E+01
CHN-YZ1-54-448.5	Not Measured	Not Measured
CHN-YZ1-55-460.5	1.838E-02	6.420E+01
CHN-YZ1-56-472.5	Not Measured	Not Measured

Table B-1.4-4 ⁵⁴Mn and ⁶⁰Co Activities for Chain in Octant ZW

Sample ID	$\mu\text{Ci/gm}$ Target Fe-54	$\mu\text{Ci/gm}$ Target Co-59
CHN-ZW2-1-4.5	Not Detected	2.887E+00
CHN-ZW2-2-10.5	1.326E-03	9.208E+00
CHN-ZW2-3-16.5	4.096E-03	2.731E+01
CHN-ZW2-4-22.5	1.405E-02	4.160E+01
CHN-ZW2-5-34.5	2.841E-02	3.040E+01
CHN-ZW2-6-46.5	4.377E-02	3.432E+01
CHN-ZW2-7-58.5	6.129E-02	4.450E+01
CHN-ZW2-8-64.5	7.787E-02	5.156E+01
CHN-ZW2-9-70.5	8.681E-02	6.096E+01
CHN-ZW2-10-76.5	1.108E-01	7.193E+01
CHN-ZW2-11-82.5	1.492E-01	8.667E+01
CHN-ZW2-12-94.5	2.661E-01	1.181E+02
CHN-ZW2-13-106.5	4.514E-01	1.476E+02
CHN-ZW2-14-118.5	8.068E-01	1.769E+02
CHN-ZW2-15-124.5	9.219E-01	1.962E+02
CHN-ZW2-16-130.5	1.188E+00	2.152E+02
CHN-ZW2-17-136.5	1.349E+00	2.288E+02
CHN-ZW2-18-142.5	1.571E+00	2.405E+02
CHN-ZW2-19-148.5	1.675E+00	2.458E+02
CHN-ZW2-20-154.5	1.896E+00	2.462E+02
CHN-ZW2-21-160.5	1.989E+00	2.475E+02
CHN-ZW2-22-166.5	2.052E+00	2.395E+02

Table B-1.4-4 (Cont'd) ⁵⁴Mn and ⁶⁰Co Activities for Chain in Octant ZW

Sample ID	$\mu\text{Ci/gm Target Fe-54}$	$\mu\text{Ci/gm Target Co-59}$
CHN-ZW2-23-172.5	2.208E+00	2.423E+02
CHN-ZW2-24-178.5	2.151E+00	2.492E+02
CHN-ZW2-25-184.5	2.276E+00	2.525E+02
CHN-ZW2-26-190.5	2.318E+00	2.473E+02
CHN-ZW2-27-196.5	2.255E+00	2.557E+02
CHN-ZW2-28-202.5	2.366E+00	2.578E+02
CHN-ZW2-29-208.5	2.296E+00	2.555E+02
CHN-ZW2-30-214.5	2.307E+00	2.502E+02
CHN-ZW2-31-220.5	2.291E+00	2.477E+02
CHN-ZW2-32-226.5	2.259E+00	2.369E+02
CHN-ZW2-33-232.5	2.101E+00	2.507E+02
CHN-ZW2-34-238.5	1.967E+00	2.597E+02
CHN-ZW2-35-244.5	1.847E+00	2.620E+02
CHN-ZW2-36-250.5	1.736E+00	2.555E+02
CHN-ZW2-37-256.5	1.500E+00	2.474E+02
CHN-ZW2-38-262.5	1.331E+00	2.354E+02
CHN-ZW2-39-268.5	1.090E+00	2.226E+02
CHN-ZW2-40-280.5	7.284E-01	2.022E+02
CHN-ZW2-41-292.5	4.871E-01	1.819E+02
CHN-ZW2-42-304.5	3.191E-01	1.591E+02
CHN-ZW2-43-316.5	2.257E-01	1.384E+02
CHN-ZW2-44-328.5	1.782E-01	1.209E+02

Table B-1.4-4 (Cont'd) ^{54}Mn and ^{60}Co Activities for Chain in Octant ZW

Sample ID	$\mu\text{Ci/gm Target Fe-54}$	$\mu\text{Ci/gm Target Co-59}$
-----------	--------------------------------	--------------------------------

CHN-ZW2-45-340.5	9.809E-02	1.096E+02
CHN-ZW2-46-352.5	9.543E-02	1.001E+02
CHN-ZW2-47-364.5	6.809E-02	9.224E+01
CHN-ZW2-48-376.5	4.997E-02	8.739E+01
CHN-ZW2-49-388.5	4.036E-02	8.362E+01
CHN-ZW2-50-400.5	2.808E-02	7.930E+01
CHN-ZW2-51-412.5	3.262E-02	7.763E+01
CHN-ZW2-52-424.5	2.823E-02	7.593E+01
CHN-ZW2-53-436.5	2.308E-02	7.549E+01
CHN-ZW2-54-448.5	2.248E-02	7.539E+01
CHN-ZW2-55-460.5	Not Measured	Not Measured
CHN-ZW2-56-472.5	Not Measured	Not Measured

Table B-1.4-5 Activity of Chain Segments Irradiated in "Pill Boxes"

Location	Shielded	$\mu\text{Ci } ^{54}\text{Mn}/\text{gram}$ ^{54}Fe	$\mu\text{Ci } ^{60}\text{Co}/\text{gram}$ ^{59}Co
C3	Yes	7.073E-02	3.646E+01
E2	No	1.401E+00	1.869E+02
E3	Yes	1.313E+00	8.232E+01
H2	No	2.352E+00	2.820E+02
H5	Yes	2.373E+00	1.212E+02
J2	No	2.826E+00	3.288E+02
K2	No	2.738E+00	3.281E+02
L1	No	2.984E+00	3.191E+02
L4	Yes	2.930E+00	1.239E+02

Table 5-4.2-1 Helium Concentrations in Beryllium HAFMs ${}^9\text{Be} (n, \alpha) {}^6\text{Li}$

Sample	Specimen Mass (mg)	Measured ${}^4\text{He}$ (10^{11} atoms)	Helium Concentration (appb) ^(a)		
			Measured	Corrected ^(b)	Average
DB-BEC-1/1 -1/3	2.71 3.52	1.582 2.008	0.8736 0.8537	0.820 0.800	0.81
DB-BEC-2/4 -2/5	1.89 2.50	2.056 2.705	1.628 1.619	1.57 1.56	1.57
DB-BEC-3/7 -3/9	3.02 2.21	2.730 2.063	1.353 1.397	1.30 1.34	1.32
DB-BEC-4/10 -4/12	2.68 2.86	0.222 0.264	0.124 0.138	0.072 0.086	0.08
DB-BEC-5/13 -5/15	3.35 2.66	2.979 2.419	1.331 1.361	1.28 1.31	1.30
DB-BEC-6/17 -6/18	2.69 2.53	3.181 2.947	1.770 1.743	1.71 1.69	1.70
DB-BEC-7/20 -7/21	2.73 2.26	2.731 2.261	1.497 1.497	1.44 1.44	1.44
DB-BEC-8/22 -8/23	1.82 1.66	2.312 2.015	1.901 1.817	1.85 1.76	1.81
DB-BEC-9/26 -9/27	2.14 1.77	0.175 0.098	0.122 0.083	0.072 0.033	0.05
DB-BEC-10/28 -10/30	1.77 2.06	1.815 2.105	1.535 1.529	1.48 1.47	1.48
DB-BEC-11/32 -11/33	1.72 1.95	2.145 2.349	1.866 1.803	1.81 1.75	1.78

^(a) Helium concentration in atomic parts per billion (10^{-9} atom fraction) with respect to the number of beryllium atoms in the specimen.

^(b) Corrected for measured helium concentration in unirradiated beryllium (0.05 appb), and from helium generation in boron impurity.

Table B-4.2-2 Helium Concentrations in Al-Li HAFMS ${}^6\text{Li} (n, \alpha) {}^3\text{H}$

Sample	Specimen Mass (mg)	Measured ${}^4\text{He}$ (10^{11} atoms)	Helium Concentration (appm) ^(a)	
			Measured	Average
DB-Li-1A	0.723	4.534	0.9034	0.897
-1B	0.609	3.765	0.8906	
DB-Li-2A	0.798	1.484	0.2679	0.270
-2B	0.609	1.147	0.2713	
DB-Li-3A	0.753	5.218	0.9982	1.010
-3B	0.583	4.135	1.022	
DB-Li-4A	0.757	3.209	0.6106	0.618
-4B	0.728	3.156	0.6245	
DB-Li-5A	0.667	0.332	0.0717	0.070
-5B	0.667	0.313	0.0676	
DB-Li-6A	0.671	4.296	0.9223	0.910
-6B	0.568	3.540	0.8978	
DB-Li-7B	0.567	3.695	0.9387	0.928
-7C	0.596	3.799	0.9182	
DB-Li-8A	0.668	4.305	0.9284	0.928
-8B	0.701	4.514	0.9276	
DB-Li-9A	0.739	4.979	0.9705	0.970
-9B	0.639	4.299	0.9691	
DB-Li-10A	0.669	4.585	0.9870	0.986
-10B	0.673	4.603	0.9852	
DB-Li-12A	0.641	4.313	0.9693	0.963
-12B	0.556	3.695	0.9573	

^(a) Helium concentration in atomic parts per million (10^{-6} atom fraction) with respect to the number of ${}^6\text{Li}$ atoms in the specimen.

Appendix C **Calculational Perturbation Factors for Dosimetry**

The Semi - Empirical BUGLE-80 fluence methodology that FTI had developed in 1990 was used to determine calculational perturbation factors for the DORT models. This appendix list these factors. They are calculational factors used to appropriately modify the calculational results for the dosimetry activities. The procedures for determining the factors are discussed in Section 3.2.

Table C.1 Perturbation Factors for ^{54}Fe (n, p) ^{54}Mn

Holder	P_{BEAMS}	P_{INST}	P_{TOTAL}
D1	.946	1.010	.955
D2	.946	1.010	.955
D4	.946	1.010	.955
D5	.946	1.010	.955
E1	.946	1.010	.955
E4	.946	1.010	.955
E5	.946	1.010	.955
F1	.980	1.000	.980
F3	.982	1.000	.982
F5	.984	1.000	.984
G1	.988	1.000	.988
G2	.988	1.000	.988
G5	.986	1.000	.986
H1	.964	1.000	.964
H4	.972	1.000	.972
J1	.980	1.024	1.003
J3	.982	1.024	1.006
J4	.983	1.024	1.007
K2	.987	1.024	1.011
K3	.987	1.024	1.011
K5	.985	1.024	1.010
M1	.985	1.000	.985
M2	.986	1.000	.986
M3	.986	1.000	.986

Table C.1 (Cont'd) Perturbation Factors for ^{54}Fe (n, p) ^{54}Mn

Holder	P_{BEAMS}	P_{INST}	P_{TOTAL}
M4	.987	1.000	.987
M5	.987	1.000	.987
N2	.983	1.000	.983
N3	.981	1.000	.981
P1	.960	1.000	.960
P2	.956	1.000	.956
Q1	.864	1.000	.864
Q2	.876	1.000	.876
Q3	.897	1.000	.897
Q4	.904	1.000	.904
S1	.978	1.000	.978
S3	.974	1.000	.974
S5	.972	1.000	.972
T1	.988	1.000	.988
T2	.988	1.000	.988
T4	.989	1.000	.989
T5	.990	1.000	.990
U4	.985	1.000	.985

Table C.2 Perturbation Factors for ^{58}Ni (n, p) ^{58}Co

Holder	P_{BEAMS}	P_{INST}	P_{TOTAL}
D4	.954	1.006	.960
D5	.954	1.006	.960
F3	.985	1.000	.985
F5	.986	1.000	.986
G5	.988	1.000	.988
J5	.986	1.015	1.001
K1	.989	1.015	1.004
M3	.988	1.000	.988
M4	.988	1.000	.988
N3	.985	1.000	.985
N4	.985	1.000	.985
P4	.962	1.000	.962
P5	.958	1.000	.958
Q3	.920	1.000	.920
S3	.977	1.000	.977
S5	.974	1.000	.974
T4	.990	1.000	.990
T5	.990	1.000	.990
U4	.987	1.000	.987

Table C.3 Perturbation Factors for $^{63}\text{Cu} (n, \alpha) ^{60}\text{Co}$

Holder	P_{BEAMS}	P_{INST}	P_{TOTAL}
D4	.968	1.006	.973
D5	.968	1.006	.973
F3	.988	1.000	.988
F5	.988	1.000	.988
G5	.989	1.000	.989
K3	.989	1.014	1.003
M3	.989	1.000	.989
M4	.989	1.000	.989
N3	.987	1.000	.987
Q3	.920	1.000	.920
S3	.986	1.000	.986
S5	.985	1.000	.985
T4	.990	1.000	.990
T5	.990	1.000	.990
U4	.989	1.000	.989

Table C.4 Perturbation Factors for $^{46}\text{Ti} (n, p) ^{46}\text{Sc}$

Holder	P_{BEAMS}	P_{INST}	P_{TOTAL}
D5	.957	1.009	.966
F5	.986	1.000	.986
G5	.988	1.000	.988
K1	.989	1.023	1.011
M3	.988	1.000	.988
S5	.979	1.000	.979
T4	.989	1.000	.989

Table C.5 Perturbation Factors for $^9\text{Be} (n, \alpha) - \text{Be HAFM}$

Holder	P_{BEAMS}	P_{INST}	P_{TOTAL}
E4	.944	1.010	.953
F3	.983	1.000	.983
H4	.975	1.000	.975
J3	.983	1.025	1.008
Q3	.920	1.000	.920
Q5	.936	1.000	.936
T5	.990	1.000	.990

Table C.6 Perturbation Factors for ^{238}U (D, f) Either ^{137}Cs or SSTRs

Holder	P_{BEAMS}	P_{INST}	P_{TOTAL}
D5	.957	0.998	.955
F4	.985	1.000	.985
F5	.986	1.000	.986
G5	.988	1.000	.988
H5	.977	1.000	.977
J5	.986	0.995	.981
K4	.988	0.995	.983
L1	.989	1.000	.989
L4	.989	1.000	.989
L5	.989	1.000	.989
M3	.988	1.000	.988
M4	.988	1.000	.988
N4	.982	1.000	.982
P4	.943	1.000	.943
P5	.937	1.000	.937
S4	.973	1.000	.973
S5	.972	1.000	.972
T4	.989	1.000	.989
U4	.985	1.000	.985

Table C.7 Perturbation Factors for ^{237}Np (n, f) Either ^{137}Cs or SSTRs

Holder	P_{BEAMS}	P_{INST}	P_{TOTAL}
D5	1.017	0.984	1.001
F4	1.010	1.000	1.010
F5	1.010	1.000	1.010
G5	1.010	1.000	1.010
H5	1.009	1.000	1.009
J5	1.009	0.960	0.969
K4	1.009	0.960	0.969
L5	1.010	1.000	1.010
M3	1.009	1.000	1.009
M4	1.010	1.000	1.010
N4	1.009	1.000	1.009
N5	1.009	1.000	1.009
P4	0.962	1.000	0.962
P5	0.958	1.000	0.958
S4	0.999	1.000	0.999
S5	0.999	1.000	0.999
T4	1.009	1.000	1.009
U4	1.007	1.000	1.007

Table C.8 Perturbation Factors for $^{59}\text{Co} (\alpha, \gamma) ^{60}\text{Co}$

Bare				Covered			
Holder	P _{BEAMS}	P _{INST}	P _{TOTAL}	Holder	P _{BEAMS}	P _{INST}	P _{TOTAL}
D1	.782	1.095	.856	D4	.890	1.039	.925
D2	.782	1.095	.856	D5	.890	1.039	.925
E1	.782	1.095	.856	E4	.890	1.039	.925
F1	.893	1.000	.893	E5	.890	1.039	.925
G1	.897	1.000	.897	F3	.946	1.000	.946
G2	.896	1.000	.896	F5	.946	1.000	.946
H1	.885	1.000	.885	G5	.947	1.000	.947
J1	.893	1.238	1.106	H4	.940	1.000	.940
K2	.893	1.238	1.110	J3	.946	1.098	1.039
M1	.899	1.000	.899	J4	.946	1.098	1.039
M2	.899	1.000	.899	J5	.947	1.098	1.040
N2	.890	1.000	.890	K3	.948	1.098	1.041
P1	.887	1.000	.887	K5	.947	1.098	1.040
P2	.887	1.000	.887	M3	.950	1.000	.950
Q1	.877	1.000	.877	M4	.950	1.000	.950
Q2	.878	1.000	.878	M5	.950	1.000	.950
S1	.897	1.000	.897	N3	.943	1.000	.943
T1	.900	1.000	.900	N4	.944	1.000	.944
T2	.900	1.000	.900	P4	.940	1.000	.940
				P5	.939	1.000	.939
				Q3	.936	1.000	.936
				Q4	.938	1.000	.938

Table C.8 (Cont'd) Perturbation Factors for $^{59}\text{Co} (\alpha, \gamma) ^{60}\text{Co}$

Bare			Covered				
Holder	P _{BEAMS}	P _{INST}	P _{TOTAL}	Holder	P _{BEAMS}	P _{INST}	P _{TOTAL}
				S3	.948	1.000	.948
				S5	.948	1.000	.948
				T4	.950	1.000	.950
				T5	.950	1.000	.950
				U4	.949	1.000	.949

Table C.9 Perturbation Factors for ^{109}Ag (n, γ) ^{110m}Ag

Bare			Covered				
Holder	P_{BEAMS}	P_{INST}	P_{TOTAL}	Holder	P_{BEAMS}	P_{INST}	P_{TOTAL}
D1	.839	1.053	.883	G5	.932	1.000	.932
G1	.923	1.000	.923	M3	.934	1.000	.934
K1	.923	1.132	1.045				
M1	.924	1.000	.924				
T1	.925	1.000	.925				

Table C.10 Perturbation Factors for ^{235}U (n, f) Either ^{137}Cs or SSTRs

Bare			Covered				
Holder	P_{BEAMS}	P_{INST}	P_{TOTAL}	Holder	P_{BEAMS}	P_{INST}	P_{TOTAL}
D2	0.705	1.144	0.807	D5	0.886	1.038	0.920
F2	0.854	1.000	0.854	F4	0.944	1.000	0.944
L2	0.865	1.000	0.865	K4	0.945	1.094	1.034
N1	0.856	1.000	0.856	L5	0.948	1.000	0.948
S2	0.859	1.000	0.859	N4	0.940	1.000	0.940
				S4	0.946	1.000	0.946
				T4	0.948	1.000	0.948
				U4	0.947	1.000	0.947

Table C.11 Perturbation Factors for ^{239}Pu (α, f) SSTRs

Bare			Covered				
Holder	P_{BEAMS}	P_{INST}	P_{TOTAL}	Holder	P_{BEAMS}	P_{INST}	P_{TOTAL}
D2	0.694	1.151	0.799	D5	0.872	1.042	0.909
F2	0.849	1.000	0.849	F4	0.937	1.000	0.937
L2	0.860	1.000	0.860	L5	0.942	1.000	0.942
N1	0.845	1.000	0.845	N4	0.933	1.000	0.933
S2	0.854	1.000	0.854	S4	0.939	1.000	0.939
				U4	0.940	1.000	0.940

Table C.12 Perturbation Factors for ^{93}Nb (α, α') $^{93\text{m}}\text{Nb}$

Holder	P_{Beams}	P_{Inst}	P_{Total}
E4	1.006	0.986	0.992
F3	1.007	1.000	1.007
F5	1.008	1.000	1.008
H4	1.006	1.000	1.006
J3	1.007	0.966	0.973
K3	1.009	0.966	0.973
Q3	0.922	1.000	0.922
Q5	0.938	1.000	0.938
S4	0.996	1.000	0.996
S5	0.995	1.000	0.995
T5	1.009	1.000	1.009